

Properties of H II Regions in the Centers of Nearby Galaxies

Luis C. Ho

Department of Astronomy, University of California, Berkeley, CA 94720-3411

and

Harvard-Smithsonian Center for Astrophysics, 60 Garden St., Cambridge, MA 02138¹

Alexei V. Filippenko

Department of Astronomy, University of California, Berkeley, CA 94720-3411

and

Wallace L. W. Sargent

Palomar Observatory, 105-24 Caltech, Pasadena, CA 91125

ABSTRACT

As part of an optical spectroscopic survey of nearby, bright galaxies, we have identified a sample of over 200 emission-line nuclei having optical spectra resembling those of giant extragalactic H II regions. Such “H II nuclei,” powered by young, massive stars, are found in a substantial fraction of nearby galaxies, especially those of late Hubble type. This paper summarizes the observational characteristics of H II nuclei, contrasts the variation of their properties with Hubble type, and compares the nuclear H II regions with those found in galaxy disks. Similarities and differences between H II nuclei and luminous starburst nuclei are additionally noted.

Nuclei in early-type spirals (S0–Sbc) on average have low excitation, and hence high oxygen abundance (from ~ 1.1 to 3.3 times the solar value), whereas those in late-type systems (Sc–I0) have excitations spanning a wide range (corresponding to less than 0.25 to 3.5 times the solar oxygen abundance). The H α luminosities of early-type nuclei greatly exceed those of later types. The enhancement of massive star formation may be linked to the higher efficiency with which bars can drive gaseous inflow in systems with prominent bulges. The early-type systems also have higher amounts of internal extinction and higher electron densities.

The physical properties of H II nuclei resemble those of giant H II regions in spiral disks in some ways, but differ in several others. The two groups emit comparable H α luminosities and generally have similar electron densities. Because of their unique

¹Present address.

location in the galaxies, nuclear H II regions are characterized by much higher oxygen abundances. H II nuclei systematically emit stronger low-ionization forbidden lines than disk H II regions, confirming a trend recognized by Kennicutt, Keel, and Blaha. We discuss several possibilities for the origin of the spectral variations.

Subject headings: galaxies: nuclei — galaxies: starburst — ISM: abundances — ISM: H II regions — stars: formation

1. Motivation

The study of extragalactic H II regions provides underpinnings for a number of astrophysical problems, such as basic understanding of the formation of massive stars, interpretation of the observed abundance patterns in the disks of spiral galaxies, and determination of the primordial helium abundance and its cosmological implications (Dinerstein 1990; Shields 1990). The majority of observations have concentrated on the most luminous nebulae (so-called giant extragalactic H II regions) located either in relatively metal-poor dwarf irregular galaxies (e.g., French 1980; Kunth & Sargent 1983; Terlevich et al. 1991) or in the disks of spirals of intermediate to late Hubble type (e.g., McCall, Rybski, & Shields 1985). As the dominant forbidden emission lines at optical wavelengths tend to decrease in strength with increasing metallicity, comparatively few H II regions have been studied systematically in early-type spirals (Oey & Kennicutt 1993), and fewer still in the central regions of galaxies. Optical emission lines are nearly ubiquitous in galactic nuclei (Keel 1983; Ho, Filippenko, & Sargent 1997b), with the majority of the spectra in late-type spirals resembling low-excitation disk H II regions (Turnrose 1976; Heckman 1980a; Keel 1983; Ho et al. 1997b). Although these “H II nuclei” are generally much more feeble in their power output than *bona fide* starburst nuclei (Balzano 1983), they can serve as convenient probes of massive star formation in the unique environment of galactic nuclei. The relatively large number of such nuclei in nearby galaxies also permits more detailed inquiries into systematic variations of physical properties with host galaxy parameters. One might gain additional insight into the nature of H II nuclei by direct comparison with disk H II regions, whose properties are better understood.

The most widely available sources of H II nuclei, until recently, are the optical spectroscopic surveys of nearby galaxies published by Heckman, Balick, & Crane (1980), Stauffer (1982), and Keel (1983). Kennicutt, Keel, & Blaha (1989; hereafter KKB) compiled all the then available data, supplemented with a few new observations, and summarized their salient observed properties. KKB found that H II nuclei generally have integrated properties, such as sizes, H α luminosities, reddening, and electron densities, comparable to those of disk H II regions, although the two classes of nebulae differ in other important aspects.

Using a large, homogeneous sample of H II nuclei extracted from a newly completed survey, we summarize the statistics of these objects, examine systematic variations of observed properties

as a function of host galaxy type, and draw appropriate comparisons with disk H II regions. A preliminary form of this study was presented in Ho, Filippenko, & Sargent (1996).

2. The New Survey

An optical spectroscopic survey of the nuclei of bright, nearby galaxies has recently been completed (Ho, Filippenko, & Sargent 1995). High signal-to-noise ratio, moderate-resolution (100–200 km s⁻¹), long-slit spectra were obtained with the Hale 5 m reflector at Palomar Observatory (Filippenko & Sargent 1985). The sample is defined to be all galaxies listed in the Revised Shapley-Ames Catalog of Bright Galaxies (Sandage & Tammann 1981) with $\delta > 0^\circ$ and $B_T \leq 12.5$ mag; it is nearly statistically complete and contains 486 galaxies spanning all morphological types. The selection criteria and the relatively large number of objects surveyed ensure that the sample provides a fair representation of the local ($z \approx 0$) galaxy population, at least for high-surface brightness systems. The observations were taken largely with a 2'' slit, and one-dimensional spectra were extracted using an aperture of 2'' \times 4'', corresponding to physical dimensions of $\sim 200 \times 400$ pc² for the typical distances of the sample galaxies (18 Mpc; Ho, Filippenko, & Sargent 1997a).² The reader may consult Ho et al. (1995) for full details of the observations, data reductions, and presentation of the spectra, Ho et al. (1997a) for the actual measurements and other quantities used in the present analysis, and Ho et al. (1997b) for further discussion concerning the statistical properties of the emission-line objects.

Following standard practice (Baldwin, Phillips, & Terlevich 1981; Veilleux & Osterbrock 1987), we identified the dominant ionization mechanism of each nucleus according to the intensity ratios of several prominent optical emission lines (Ho et al. 1997a). H II nuclei are defined to be objects whose spectra look similar to those of H II regions, and hence their primary source of ionization is assumed to be photoionization by ultraviolet radiation from young, massive stars. Between 4200 and 6900 Å, the wavelength range covered in our survey, the strongest emission lines observed in H II nuclei are the hydrogen recombination lines (H γ , H β , and H α) and [O III] $\lambda\lambda 4959, 5007$. The strength of [O III] relative to the hydrogen lines spans a wide range depending on the excitation of the gas. The low-ionization transitions of [N II] $\lambda\lambda 6548, 6583$, [S II] $\lambda\lambda 6716, 6731$, and especially [O I] $\lambda\lambda 6300, 6363$ are normally quite weak compared to H α ; indeed, this trait is the primary characteristic used to distinguish H II nuclei from active galactic nuclei (AGNs). The sensitivity of our survey, however, is sufficiently high that we almost always detect [N II] and [S II], and we can measure [O I] in the majority (> 80%) of the objects. In total, 206 H II nuclei were detected in the Palomar survey, of which $\sim 80\%$ were observed under photometric conditions.

It is important to recognize that our data, as presented here, contain only limited spatial information. Imaging studies of emission-line nuclei (e.g., Pogge 1989) have shown that

²We adopt $H_0 = 75$ km s⁻¹ Mpc⁻¹ in this series of papers.

star-forming nuclei often exhibit complicated and sometimes extended patterns of line emission. Without imaging data with sufficient angular resolution, it is virtually impossible to define nuclear H II regions as single, discrete entities. The spectra were extracted using an aperture of fixed angular size projected onto the sky; this corresponds to varying physical dimensions depending on the distance of the galaxy. As emphasized by Ho et al. (1997a), the emission-line measurements of individual objects in our survey may carry substantial uncertainty. If the line-emitting material is much more extended than our observation aperture, we will underestimate the flux. For more compact emission, the integrated light may originate from a number of discrete, and possibly overlapping, regions, and the flux for a single region will be overestimated. On the other hand, the *statistical* properties of large numbers of objects should be much more reliable, as individual fluctuations will average out. We proceed with our analysis in the next section with this principle in mind.

In order to contrast typical H II nuclei with their more luminous counterparts, we collected spectroscopic measurements for starburst nuclei from the literature. Objects classified as starburst nuclei generally having nuclear H α luminosities greater than 10^{40} ergs s $^{-1}$ (e.g., Balzano 1983). Thus, in compiling data for the present purpose, we arbitrarily used this luminosity cut-off. We found forbidden-line intensities for 62 objects in French (1980), Balzano (1983), and Veilleux & Osterbrock (1987), and H α luminosities for 98 objects in Balzano (1983). Balzano selected her sample from the survey of Markarian and his colleagues (Mazzarella & Balzano 1986, and references therein).

Data for disk H II regions are more readily available. Spectroscopically measured line-intensity ratios for about 200 H II regions in spiral disks were taken from the studies of McCall et al. (1985) and Ryder (1995), and line measurements for a small number of regions in dwarf irregular galaxies were used to supplement the low-metallicity end of the H II-region sequence (French 1980; Dinerstein & Shields 1986). The study of Kennicutt (1988) furnished H α luminosities for 95 first-ranked disk H II regions selected from a wide distribution of galaxy morphological types.

3. Basic Properties of Nuclear H II Regions

3.1. Statistics and Host Galaxies

A detailed discussion of the detection rate of the emission-line nuclei in our survey, including that of H II nuclei, can be found in Ho et al. (1997b; see also Ho 1996). In brief, H II nuclei constitute 42% of all galaxies brighter than $B_T = 12.5$ mag. Late-type galaxies contain H II nuclei much more frequently than early-type galaxies. Up to 80% of the galaxies with Hubble type between from Sc and Im have an H II classification, to be compared with 51% for Sb, 22% for Sa, and 8% for S0. We found no ellipticals with an H II nucleus in our sample.

The galaxies hosting H II nuclei tend to be less luminous than those hosting AGNs (Ho et al.

1997b), as one would expect from the correlation between nuclear type and galaxy morphology. Our subsequent analysis will frequently contrast early-type and late-type systems, where “early” here refers to types ranging from S0 to Sbc and “late” corresponds to Sc through I0. A small number (6) of galaxies with peculiar classifications were omitted. We show in Figure 1, for later reference, the absolute magnitudes of these two groups; as is well known (e.g., Roberts & Haynes 1994), late-type galaxies clearly have lower luminosities, although there is considerable overlap between the two groups.

Roughly 50%–60% of the disk galaxies in the survey are barred, consistent with the bar fraction in the general field galaxy population (Ho et al. 1997a). Considerations of the dynamical influence of a bar on the gaseous component of the disk predict that barred systems should show enhanced star formation in their centers. While the incidence of H II nuclei is evidently not higher in the expected sense, we do find evidence for an increased star-formation rate in the barred sample (Ho, Filippenko, & Sargent 1997c). As discussed in greater detail in that paper, bars in early-type spirals seem to exert the greatest impact on nuclear star formation, while their effect in late-type systems is relatively minor.

3.2. $H\alpha$ Luminosity and $H\beta$ Equivalent Width

The $H\alpha$ luminosities³ [$L(H\alpha)$] of H II nuclei span an enormous range ($L(H\alpha) \approx 2 \times 10^{36} - 4 \times 10^{41}$ ergs s^{-1} ; median = 1.6×10^{39} ergs s^{-1}), with the upper end partly overlapping with starburst nuclei (Fig. 2). The lower end of the luminosity distribution undoubtedly suffers from severe selection biases, which themselves must depend on Hubble type, as it becomes progressively more difficult to detect weak emission lines superposed on the bright stellar background of the bulge. Compared with late-type (Sc–I0) galaxies, early-type (S0–Sbc) systems have nuclei with much higher $H\alpha$ luminosities; the increase in the median $L(H\alpha)$ is about a factor of 9. The cumulative distributions of the two samples differ very significantly according to the Kolmogorov-Smirnov (K-S) test (Press et al. 1986); the probability (P_{KS}) that the two distributions are drawn from the same population is 1.9×10^{-5} . Although the median distance of the early-type group (21.5 Mpc) is 30% larger than that of the late-type group (16.9 Mpc), this effect alone probably cannot account for the large difference in $L(H\alpha)$ between the two. If the surface brightness of $H\alpha$ emission were constant in

³Recall the caveat mentioned in § 2 that our emission-line measurements refer only to the limited, distance-dependent spatial scale sampled by the narrow slit of the observations. In this comparison, we assume that both the $H\alpha$ luminosities and equivalent widths are representative of H II nuclei in a statistical sense. For spatially resolved nebulae, the emission will be underestimated by an amount which depends on the spatial variation of the line emissivity. Although the individual emission-line parameters are probably inaccurate, it is hoped that the ensemble properties will be representative of the class as a whole. The $H\alpha$ luminosities of the starburst nuclei should be fairly reliable, since Balzano (1983) selected them based on their semi-stellar appearance, and the fluxes were measured through either a $3'' \times 8''$ aperture or a $4''$ round aperture. Similarly, Kennicutt (1988) obtained aperture photometry for the first-ranked disk H II regions, which should yield accurate integrated $H\alpha$ fluxes.

the central regions of both groups, $L(\text{H}\alpha)$ in the early-type galaxies would be only $\sim 70\%$ higher. This is a realistic upper limit to the distance-induced enhancement, since in most cases the $\text{H}\alpha$ emission should be more centrally concentrated. Instead, the increase of $L(\text{H}\alpha)$ among early types most likely can be attributed to enhancement of central star formation resulting from bar-driven gas inflow, an effect observed *only* in early-type systems (Ho et al. 1997c).

First-ranked disk H II regions have luminosities intermediate between those of early- and late-type H II nuclei, most closely matching nuclei in Sc–Scd hosts. But, as found by KKB, H II nuclei on the whole do not differ appreciably from disk H II regions in terms of $\text{H}\alpha$ luminosity.

We confirm that H II nuclei have much smaller Balmer emission-line equivalent widths than do disk H II regions (KKB). [In this comparison we use the equivalent width of $\text{H}\beta$ instead of $\text{H}\alpha$ because the latter was not given in the literature sources we chose. $\text{EW}(\text{H}\beta)$ is not tabulated in our data base, but it can be calculated easily from the information given in Ho et al. (1997a).] This primarily underscores the difference in the underlying stellar population between the two classes of objects, since it has been shown that the emission-line luminosities are comparable. The optical stellar continuum in galactic nuclei predominantly comes from red, evolved stars. With the exception of the nuclei in very late-type hosts, the median equivalent width of $\text{H}\beta$ emission shows little variation among Hubble types (Fig. 3), being typically 4–5 Å. The tail in the Sc–I0 distribution, which reaches values as high as 350 Å, is due almost entirely to Sd–Im galaxies and closely resembles the distribution for disk H II regions. This is hardly surprising, considering that optically distinct “nuclei” very rarely exist in galaxies of such late Hubble types. The central regions of such objects are seldom well-defined (Ho et al. 1995), and, during the spectral extractions, we usually chose the intensity peak closest to the center of the slit to represent the “nucleus.” Undoubtedly many or most such nuclei are counterparts of giant H II regions observed in irregular galaxies and in the disks of late-type spirals.

The relatively low $\text{H}\alpha$ luminosities of H II nuclei suggest that in general the centers of nearby galaxies experience only one-hundredth the amount of star formation taking place in rarer, more distant starburst nuclei. Indeed, the low Balmer-line equivalent widths observed are consistent with the picture that these objects have been forming stars essentially at a constant rate of a few percent of a solar mass per year over the age of the disk (KKB).

3.3. Reddening

As emphasized by KKB and readdressed recently by Shields & Kennicutt (1995), dust can have a considerable impact on the structure and on the thermal and ionization balance of an H II region. The effect is expected to be particularly large in the regime of high (\gtrsim solar) metallicity, which, as will be shown below, typifies most galactic nuclei. Figure 4 illustrates that both H II nuclei and disk H II regions suffer nonnegligible amounts of extinction as gauged by comparison of the observed and predicted hydrogen Balmer decrement. With the exception of a small number

of objects having unusually high reddening (IC 10, NGC 891, NGC 1569, M82), the dispersion in the distribution of reddening is comparable for H II nuclei and disk H II regions. H II nuclei do have somewhat higher reddening: the median values of $E(B - V)$ are 0.54, 0.35, and 0.42 mag for early-type, late-type, and all nuclei combined, respectively. This is to be compared with 0.29 mag for disk H II regions. Performing a K-S test on these distributions indicates that the difference between disk H II regions and late-type nuclei is insignificant ($P_{\text{KS}} = 0.29$), but highly significant when compared to early-type nuclei ($P_{\text{KS}} = 0.0022$).

We draw attention to a minor caveat to the above discussion. It is possible that the apparently higher reddenings in early-type H II nuclei may result from an unknown source of systematic error in the measurement of the Balmer decrement. The equivalent widths of the Balmer emission lines are inherently small (§ 3.2), and accurate measurement is all the more challenging in early-type galaxies because of the strong stellar continuum. The $H\beta$ line poses more difficulty than $H\alpha$ for a number of reasons (Ho et al. 1997a) and therefore it carries a larger uncertainty, although we can think of no obvious reason why its intensity might have been systematically underestimated in early-type galaxies. As an illustration of the pitfalls of not properly accounting for the stellar absorption, we note that the distribution of internal reddening in H II nuclei obtained by Véron & Véron-Cetty (1986) peaks near 0.8 mag, substantially higher than our value of 0.42 mag. We suspect that the discrepancy can be attributed to the fact Véron & Véron-Cetty did not correct their spectra for starlight contamination.

A systematic overestimate of $E(B - V)$ for early-type nuclei will affect the quantitative details of our discussion on $H\alpha$ luminosity (§ 3.2), but is unlikely to change the general conclusions. For example, the maximum difference between the median $E(B - V)$ of early-type nuclei and disk H II regions amounts to 0.25 mag, which translates to a scaling factor of 1.8 at $H\alpha$. Similarly, the H II nuclei in early-type galaxies are reddened by 0.19 mag more than those in late-type galaxies, translating to a maximum enhancement of 60% in $H\alpha$ luminosity; this is negligible compared to the derived factor of ~ 10 difference in luminosities.

A potentially much more serious uncertainty arises from our lack of knowledge of the *total* extinction in galactic nuclei. The conventional method of using the Balmer decrement to estimate the optical extinction assumes a uniform, foreground dust screen. This is certainly a gross oversimplification for real star-forming regions, perhaps all the more so for the complex environment of galaxy nuclei. Thus, the reddenings determined from Balmer decrements should be regarded as lower limits to the true values. With the caveat that the presence of dust grains diminishes the number of ionizing photons, measurements of the free-free continuum at radio wavelengths can in principle provide a more direct measurement of the optical depth, and observations indicate that while the optical extinction in disk H II regions is usually underestimated using optical techniques, the error is generally not too large (Israel & Kennicutt 1980; Kaufman et al. 1987; van der Hulst et al. 1988). Unfortunately, the same technique has not been widely applied to galactic nuclei.

3.4. Electron Density, Ionized Hydrogen Mass, and Volume Filling Factor

Nearly all of the H II nuclei in our survey have reliable measurements of the density-sensitive [S II] $\lambda\lambda 6716, 6731$ doublet. The lines fall on a relatively uncomplicated part of the stellar continuum, and the moderately high resolution ($\sim 100 \text{ km s}^{-1}$) of our red spectra allows accurate deblending of the lines. The electron densities (n_e) were derived from the [S II] $\lambda 6716/\lambda 6731$ ratio for an electron temperature of 10^4 K and using the latest atomic parameters for S^+ (see Ho et al. 1997a). For consistency we rederived n_e for the disk H II regions in the same manner using the published [S II] intensities. The vast majority of the nuclei have [S II] ratios in the low-density limit (Fig. 5). The average density (180 cm^{-3}) and dispersion (200 cm^{-3}) for the H II nuclei in our sample are quite similar to those of the disk H II regions studied by KKB; using the average [S II] ratio given by McCall et al. (1985), for example, we find that disk regions typically have $n_e \approx 140 \text{ cm}^{-3}$. KKB, on the other hand, concluded that H II regions in nuclei on average have much higher densities than those in disks. We believe that the discrepancy probably can be traced to a subtle systematic error in the [S II] measurements of Stauffer (1982) and Keel (1983), whose surveys KKB used to compile much of their sample of H II nuclei. The source of this error has been discussed by Ho (1996).

Interestingly, the electron densities are about a factor of two larger in early-type hosts than in late-type hosts (median $n_e = 180 \text{ cm}^{-3}$ versus 80 cm^{-3}). The K-S test assigns a probability of 0.0016 that the two distributions are drawn from the same population. It seems highly unlikely that this finding is influenced by systematic errors due to measurement. As stated above, the spectral region concerned generally is unhampered by strong stellar absorption. Suppose that H II nuclei in early-type hosts have lower electron temperatures than those in late-type hosts, as might be anticipated, for example, from the inverse correlation between metal abundance and nebular temperature (e.g., Dinerstein 1990). Indeed, if we assume a lower value of T_e for early-type nuclei, n_e would decrease, but the difference persists at a significant level. Adopting $T_e = 5 \times 10^3 \text{ K}$ for early-type nuclei, for instance, decreases the median density by only $\sim 25\%$, and the K-S test yields $P_{\text{KS}} = 0.0079$ for the density distributions of the two morphological groups. Thus, it seems that H II nuclei in early-type galaxies truly do have higher electron densities than those in late-type systems. This might be a natural consequence of the different degree of bulge dominance in the two cases. Gas sitting in the deeper gravitational potential of a big bulge naturally is subject to a larger pressure which then results in a higher density. In general, the central regions of galaxies are likely to experience much higher interstellar pressures than in the disk (Spergel & Blitz 1992; Helfer & Blitz 1993). We find it somewhat surprising, therefore, that the densities deduced in the nuclear H II regions should be so similar to those in disk regions.

Following KKB, we can obtain rough estimates of the ionized hydrogen masses by combining the extinction-corrected $\text{H}\alpha$ luminosities with the electron densities. $M(\text{H II})$ varies between 10^2 to a few $\times 10^6 M_\odot$, with a median value of $\sim 10^5 M_\odot$. The disk population of giant H II regions exhibits similar characteristics (Kennicutt 1984). The H II masses in early-type nuclei are about 2–3 times larger than in late-type nuclei. Similarly, the volume filling factors can be crudely

calculated by assuming that the line-emitting material has dimensions comparable to the size of our observing aperture. This exercise yields filling factors ranging from 10^{-6} to 10^{-1} , with most of the values clustering near 10^{-5} ; no large variation with Hubble type is seen. As realized by KKB, the ionized gas in nuclear regions evidently attains a much higher degree of clumpiness than in the disk.

3.5. Line-Intensity Ratios

3.5.1. $[O\ III]/H\beta$ Ratio and Oxygen Abundances

Systematic variations among the emission-line spectra of objects hold important clues to their physical conditions. In this section, we examine several well-measured emission-line intensity ratios, paying close attention to variations among H II nuclei as a function of Hubble type, between H II nuclei and starburst nuclei, and between H II nuclei and disk H II regions. In the discussion to follow, we eliminated a small number of highly uncertain data points and upper limits. Our sample is large enough that sufficient data remained after this selection process.

Figure 6 illustrates the distributions of $[O\ III]\ \lambda 5007/H\beta$ for the different object classes. $[O\ III]/H\beta$ measures the excitation of the nebulae: “high-excitation” objects have high $[O\ III]/H\beta$, and “low-excitation” objects have low $[O\ III]/H\beta$. Since $[O\ III]\ \lambda 5007$ is an important coolant in H II regions, the ratio is primarily sensitive to, and inversely correlated with, the oxygen abundance (e.g., McCall et al. 1985; Dinerstein 1990). The $[O\ III]/H\beta$ ratio in H II nuclei spans a wide range (Fig. 6a), forming a spectral sequence mimicking the well-established one of giant H II regions (Fig. 6e). An obvious difference is that H II nuclei cluster toward the low-excitation end of the sequence, since galaxy nuclei generally have higher metallicities than disks. Not unexpectedly, the excitation varies with morphological type. Although low-excitation H II regions exist in late-type nuclei (Fig. 6c), high-excitation H II regions are not found in early-type nuclei (Fig. 6b); there appears to be a genuine dearth of high-excitation nuclei ($[O\ III]/H\beta \gtrsim 2$) in S0–Sbc galaxies.

In the absence of a direct measurement of the electron temperature, it is customary to derive the oxygen abundance in an H II region through the use of empirically calibrated intensity ratios of bright lines. A commonly used calibrator, introduced by Pagel et al. (1979), is $R_{23} \equiv ([O\ II] + [O\ III])/H\beta$. Although our spectra do not cover $[O\ II]\ \lambda 3727$, it is well established that in ionization-bounded nebulae $[O\ III]/H\beta$ correlates strongly with $[O\ II]/H\beta$, and hence with R_{23} , over a wide range of excitation (e.g., McCall et al. 1985; Zaritsky, Elston, & Hill 1990). McCall et al. show, for instance, that $[O\ III]/H\beta$ closely traces R_{23} for $0.07 \lesssim [O\ III]/H\beta \lesssim 3.7$. Exploiting this empirical fact, we use the R_{23} –O/H calibration of Edmunds & Pagel (1984), as updated by McCall et al. (1985), to estimate oxygen abundances from our $[O\ III]/H\beta$ measurements. The uncertainty of this calibration, mainly due to systematic errors, is estimated to be ~ 0.2 dex (Edmunds & Pagel 1984). The H II nuclei of early-type spirals have $[O\ III]/H\beta$ ratios ranging from ~ 0.1 to 2.0, with a median value of 0.4. The corresponding range and median value of 12 +

$\log(O/H)$ are 8.88 to 9.36 and 9.16, respectively; for a solar oxygen abundance of $12 + \log(O/H) = 8.84$ (McCall et al. 1985), these translate to 1.1 to 3.3 and 2.1 times the solar value. Late-type systems, on the other hand, exhibit $[O\ III]/H\beta$ ranging from as low as ~ 0.06 to as high as 5.5, with a median value of 0.6. The equivalent range in oxygen abundances is probably less than 0.25 to 3.5 times solar, and the median value is 1.9 times solar. The lower bound is rather uncertain because the R_{23} versus O/H calibration becomes double valued for very low values of O/H .

The morphological types of Markarian starburst nuclei are similar to those of H II nuclei, perhaps with a slightly underrepresentation of galaxies with late types (see Fig. 2 of Balzano 1983). The excitation level of starburst nuclei (Fig. 6d), on the other hand, is strikingly high (contrary to Balzano’s conclusion) compared to our sample of H II nuclei. It is tempting to interpret this finding in terms of evolution. Could starburst nuclei be the predecessors of nearby H II nuclei? This would be consistent with the higher luminosities in starbursts (Fig. 2) and the lower metal abundance implied by their higher excitation (median $[O/H] \approx [O/H]_{\odot}$).

3.5.2. “Anomalous” Strengths of the Low-Ionization Lines

We next consider the ratio $[N\ II]\ \lambda 6583/H\alpha$. Largely because these two lines are often strong, lie close in wavelength, and fall on a sensitive portion of modern CCD spectrographs, this ratio is widely used as the principal criterion to classify emission-line nuclei. Because giant H II regions virtually never exhibit $[N\ II]/H\alpha > 0.6$ (e.g., Fig. 8d), it is popular practice (e.g., Keel 1983) to adopt this as the dividing line between nuclei photoionized by stars versus those powered by nonstellar processes (i.e., AGNs). Since we have available other spectral lines in addition to these, we prefer to follow the recommendations of Veilleux & Osterbrock (1987) and base our classification also on $[S\ II]/H\alpha$ and $[O\ I]/H\alpha$ (Ho et al. 1997a). We believe this practice to be more reliable, as it mitigates possible confusion from selective abundance enhancement of nitrogen.

The distribution of H II nuclei in the $[O\ III]/H\beta$ vs. $[N\ II]/H\alpha$ plane parallels the familiar disk H II region sequence, shown in Figure 7 as solid points along with the theoretical track of McCall et al. (1985). For disk H II regions, the observed sequence is usually interpreted to reflect predominantly the hardening of the ionizing radiation field with decreasing metal abundance, although alternative explanations have been advanced (cf. McCall et al. 1985; Evans & Dopita 1985; McGaugh 1991). The most striking feature is the clear *offset* between the two classes of objects. The H II nuclei, especially those with $-1 \lesssim \log [O\ III]/H\beta \lesssim 0.5$, have *larger* $[N\ II]/H\alpha$ (by about 0.2–0.3 dex) for the same excitation. This effect was first noticed by KKB and will be discussed later. The range of line ratios is nearly a factor of two larger among H II nuclei (Fig. 8). Starburst nuclei have $[N\ II]/H\alpha$ ratios quite comparable to those of late-type H II nuclei (Fig. 8), and hence they are similarly enhanced relative to disk H II regions. Coziol et al. (1997) noticed the same trend in their sample of starbursts. Figure 9 examines in more detail the dependence of the $[N\ II]/H\alpha$ ratio on Hubble type. Early-type systems have the largest $[N\ II]/H\alpha$ ratios, especially over the range $-0.5 \lesssim \log [O\ III]/H\beta \lesssim 0.2$; this may be an indication that nitrogen is

selectively enhanced in these objects.

As with $[\text{N II}]/\text{H}\alpha$, marked differences can be seen between the $[\text{S II}]/\text{H}\alpha$ ratios of H II nuclei and disk H II regions (Fig. 10 and 11); the nuclear regions show a larger range of observed values, and they are distinctly enhanced relative to the disk objects. The magnitude of the shift is about the same as that of $[\text{N II}]/\text{H}\alpha$, on the order of 0.2–0.3 dex. A similar trend can be seen qualitatively in $[\text{O I}]/\text{H}\alpha$ (Fig. 13 and 14), although in this case there are very few measurements of $[\text{O I}]$ in disk H II regions for comparison (the data are virtually non-existent in the low-excitation regime). Nevertheless, assuming that the model predictions of McCall et al. (1985) adequately represent real H II regions, it appears that the enhancement of $[\text{O I}]$ among H II nuclei is even larger than in $[\text{N II}]$ and $[\text{S II}]$ (~ 0.5 dex for the ridge-line of the H II nuclei population). One must be cautious, however, in drawing conclusions based on observationally unverified models. The $[\text{O I}]$ line emits almost exclusively from the partially ionized transition region, which, in the case of a nebula photoionized by hot stars, is very thin and depends sensitively on the nebular structure. Campbell (1988) finds that her theoretical models of high-excitation H II regions systematically underpredict the observed $[\text{O I}]$ strengths by large factors (typically on the order of 0.5 dex; see her Fig. 4). We should also remark that $[\text{O I}]/\text{H}\alpha$ has much larger scatter at a given excitation than do $[\text{N II}]/\text{H}\alpha$ or $[\text{S II}]/\text{H}\alpha$. Surely measurement errors for this weaker line must affect the data more severely, but it is conceivable that part of the larger scatter is real, perhaps reflecting its sensitivity to geometry and to shock excitation (see § 4.2).

Variations of the $[\text{S II}]/\text{H}\alpha$ ratio with the Hubble type of H II nuclei (Fig. 12) exhibit a different behavior compared to $[\text{N II}]/\text{H}\alpha$. The nuclei in the two morphological groups have essentially the same average $[\text{S II}]/\text{H}\alpha$ values at a given excitation, with the late-type objects exhibiting a somewhat larger dispersion. The same trend may also be present in $[\text{O I}]/\text{H}\alpha$ (Fig. 13), but the larger scatter and smaller sample size make the comparison more difficult. It is noteworthy that the highest values of $[\text{S II}]/\text{H}\alpha$ and $[\text{O I}]/\text{H}\alpha$ are associated almost exclusively with late-type galaxies, a point we will return to later (§ 4.2).

4. Discussion

4.1. Enhancement of Low-Ionization Lines

One of the most interesting results of this study is the confirmation of KKB’s finding that H II nuclei systematically emit stronger low-ionization forbidden lines compared to disk H II regions. Stauffer (1981) first noticed this effect for the $[\text{N II}]/\text{H}\alpha$ ratio and suggested shock-wave heating as a possible explanation. The H II nuclei in the study of Veilleux & Osterbrock (1987), on the other hand, did not show any obvious differences with disk H II regions, probably because of the small size of the sample.

KKB argued that the most likely explanation for those nuclei showing enhancement in the

low-ionization species is that they contain a weak AGN. AGNs have harder ionizing spectra than O and B stars; for a cloud optically thick to the Lyman continuum, the high-energy photons create an extensive partially ionized zone from which low-ionization transitions such [O I], [S II], and, to a lesser extent, [N II] originate. As supporting evidence for a secondary ionization component from an AGN, KKB showed examples whose kinematic properties indicate a composite nature, although it remains to be established how common these sources are among objects classified as H II nuclei. Many genuine composite nuclei are known (e.g., Véron et al. 1981; Heckman et al. 1983; Keel 1984; Shields & Filippenko 1990), and, in fact, objects with optical spectra intermediate between those of AGNs and H II nuclei constitute a non-trivial fraction of all emission-line nuclei (Ho, Filippenko, & Sargent 1993; Ho 1996; Ho et al. 1997b). These “transition objects” generally have stronger low-ionization lines than do the objects considered here, but it is possible that an AGN component, whose strength spans a wide dynamic range, is present in *most* galaxy nuclei. Indeed, the formal dividing line between H II-like and AGN-like sources strictly speaking has no physical significance. The classification system for narrow emission-line objects (e.g., Baldwin et al. 1981; Veilleux & Osterbrock 1987; Ho et al. 1997a) is based on a set of empirical, largely *ad hoc* criteria. In this interpretation, those H II nuclei showing stronger than usual (i.e., compared to disk H II regions) low-ionization lines are simply the ones with a weak AGN component. It would be difficult to distinguish this hypothesis from other possibilities (see below) based on optical data alone. If present, the weak active nucleus may be revealed by sensitive observations at radio, ultraviolet, or X-ray wavelengths.

In connection with the hidden-AGN hypothesis, we recall that the nuclei with the most pronounced [N II] enhancement appear in early-type galaxies, precisely the variety that preferentially host definitive AGNs (Ho et al. 1997b). While this may be taken as additional evidence that a nonstellar source underlies the observed excitation patterns, we hasten to add that the [S II] and [O I] lines show just the opposite effect (they are stronger in late-type galaxies). Nitrogen might be selectively enriched in the centers of bulge-dominated galaxies.

Strong low-ionization lines also can be produced through collisional excitation by shocks. KKB considered shocks from supernova remnants (SNRs) an improbable explanation for the line-strength anomalies, as the number of SNRs required was deemed excessive, and, in any case, implies that H II regions in galactic nuclei differ in fundamental ways from those in disks. However, it does not seem unreasonable that shocks resulting from the *bulk* or *turbulent* motions of the line-emitting gas will give rise to enhanced low-ionization line strengths. The gas velocities in galactic nuclei are almost certainly supersonic and larger than those within individual, isolated disk H II regions, and noncircular motions, which can lead to cloud-cloud collisions, are not uncommon (e.g., Kenney 1996, and references therein). A cursory examination of the line intensities predicted for low-velocity shocks (e.g., Shull & McKee 1979; Ho et al. 1993) indicates that the observed “excess” can be easily accommodated.

The photoionization calculations of Filippenko & Terlevich (1992) and Shields (1992) demonstrated that O stars with high effective temperatures ($T_{eff} = 45,000\text{--}50,000$ K) in an

environment with lower than typical ionization parameter can generate strong low-ionization lines. In fact, these investigators sought to explain low-ionization nuclear emission-line regions (LINERs; Heckman 1980b) with such models. The presence of high effective stellar temperatures in the metal-rich environments of galactic nuclei ostensibly violates the known inverse correlation between T_{eff} and metallicity obeyed by disk H II regions (Shields & Tinsley 1976; McCall et al. 1985; Vílchez & Pagel 1988), but Shields (1992) and Filippenko & Terlevich (1992) speculated that nuclear H II regions may depart from this trend. That H II nuclei are required in this scenario to have systematically lower ionization parameters than disk H II regions may be consistent with our finding that the nuclear regions tend to have lower volume filling factors (§ 3.4). The ionization parameter, U , is proportional to $[Q(\text{H})nf^2]^{1/3}$, where $Q(\text{H})$ is the number of ionizing photons s^{-1} , n is the gas number density, and f is the volume filling factor. All else being equal, a smaller f leads to a smaller U .

Examination of the impact of dust grains on the thermal properties of H II regions offers perhaps a more straightforward explanation. Although Mathis (1986) concluded that dust has a minimal effect on the emergent optical spectrum of H II regions, the calculations of Shields & Kennicutt (1995) indicate that the influence can be quite appreciable under conditions characterized by higher than solar metallicity, as is the case for many H II nuclei (§ 3.5.1). Compared to the dust-free case, grains enhance optical forbidden emission by increasing the equilibrium electron temperature, principally through depletion of gas-phase coolants. We anticipate, therefore, that at least part of the spectral differences observed between disk and nuclear H II regions might be due to the effect of dust grains, so long as the higher metallicity in the nuclear H II regions is also accompanied by a higher dust content. After comparing the results of the Shields & Kennicutt photoionization models with our data (Fig. 7, 10, and 13), it is apparent that the predicted line strengths do indeed provide a reasonably good match to the observations. Shields & Kennicutt performed the same exercise using the smaller data set of KKB (which did not contain measurements of the [O I] line) and arrived at the same conclusion.

Shields & Kennicutt speculated that the higher dust content inferred in galaxy nuclei might be achieved if the gas density in these environments is elevated. The growth of grains appears to be favored in denser media, since the level of depletion of many metals increases with increasing gas density (e.g., Phillips, Gondhalekar, & Pettini 1982). Although higher gas densities in the central regions of galaxies may result directly from the high interstellar pressures present, there is no evidence of this in our data (§ 3.4). Of course, one might question whether the density of the electrons derived from the [S II] lines actually trace the density of the neutral material. The molecular clouds could have substantially higher densities than the ionized gas associated with the H II regions. Alternatively, the dust content in galactic nuclei might be enhanced as a natural consequence of the higher stellar density present, since dust forms predominantly in evolved stars (Mathis 1990). This scenario can account for the difference in internal extinction between nuclear and disk H II regions, as well as that between early-type and late-type H II nuclei (§ 3.3).

Finally, we mention the likelihood of a significant contribution to the line emission from the

“diffuse ionized gas.” This component of interstellar gas, also called the “warm ionized medium,” has long been recognized in the Galaxy (see Reynolds 1990) and is now known to be pervasive in the disks of other spirals and irregulars (e.g., Rand 1996; Greenawalt, Walterbos, & Braun 1997, and references therein). The optical spectrum of the diffuse gas exhibits characteristically low stages of ionization as indicated by strong [N II] and [S II], but [O III] and [O I] are generally very weak (e.g., Domgörgen & Mathis 1994). Thus, while the high [N II]/H α and [S II]/H α ratios in the nuclei mimic some of the spectral signatures of the diffuse ionized gas, the accompanying high values of [O I]/H α are inconsistent with such an origin. The weak [O I] line in the diffuse emission is thought to reflect the matter-bounded conditions of the emitting material (Domgörgen & Mathis 1994). The tight correlation of the [S II] and [O I] line strengths in our nuclei (Fig. 15; see also Fig. 14 in Ho et al. 1997a for a similar correlation between [N II] and [O I]), and, indeed, the mere existence of a well-defined spectral sequence in the line-intensity ratio diagrams shown in Figures 7, 10, and 13 implies that ionization-bounded conditions must prevail in nuclear H II regions, as is the case in most disk H II regions (McCall et al. 1985). We therefore think that it is highly unlikely that the observed line-ratio anomalies stem from significant contamination by the diffuse ionized gas. Lehnert & Heckman (1994) noticed that the integrated spectra of spiral galaxies in the spectrophotometric atlas of Kennicutt (1992) *also* show enhanced [N II]/H α and [S II]/H α with respect to the standard H II-region sequence, and they postulated that a sizable fraction of the integrated emission could arise from the diffuse medium. They did not, however, present data for [O I], most likely because of the difficulty in measuring this weak line in the available data. Future quantification of the [O I] strength in the integrated optical spectra of galaxies will be useful for constraining the nature of their line emission.

4.2. Evidence for Shock Excitation

Some H II nuclei in late-type hosts appear to have stronger [S II] and [O I] lines than nuclei of similar excitation in spirals of earlier type (§ 3.5.2). Unusually strong [S II] emission has previously been noticed by Peimbert & Torres-Peimbert (1992) in some “H II galaxies.” Inspecting the subsample of 15 nuclei with [S II]/H α \geq 0.5 (Fig. 11), it is apparent that the majority of them have the highest [O I]/H α ratios in the sample (median value = 0.054). This is to be expected, since the two line ratios correlate well with each other (Fig. 15), reflecting their common emission region. Most of the objects have Hubble types ranging from Scd to Sdm, have rather low luminosities (median $M_{B_T}^0 = -19.4$ mag), and are located closer than average (median distance = 11.5 Mpc). Shocks from embedded SNRs, or perhaps other forms of mechanical energy injection such as stellar winds from massive stars, are probably responsible for the enhanced [S II] and [O I] emission in these systems, although it is conceivable that photoionization from very hot stars can achieve the same effect (see § 4.1). In view of the low metallicities anticipated in such late-type nuclei, the effects of dust alone are probably insufficient. The presence of strong [O I] can further rule out the diffuse ionized gas as the main culprit. The shock hypothesis can be tested either by directly measuring a temperature-sensitive line such as [O III] λ 4363, or by attempting to detect

the SNRs themselves.

Perhaps the clearest example of a shock-excited object in our sample is IC 2574, which appears as an outlier in Figures 7 and 9. The very low excitation of the spectrum ($[\text{O III}]/\text{H}\beta = 0.23$) is very peculiar for a galaxy classified as a Magellanic spiral (SABm; Ho et al. 1997a). Indeed, Miller & Hodge (1996) have shown that the oxygen abundance of several of its bright H II regions is only about one-tenth solar, consistent with the late Hubble type of the galaxy. The three H II regions analyzed by Miller & Hodge, which do not coincide with the positions sampled by our slit, have $[\text{O III}]/\text{H}\beta$ ratios between 3 and 5. The strengths of $[\text{N II}]$ ($[\text{N II}]/\text{H}\alpha = 0.07$) and $[\text{S II}]$ ($[\text{S II}]/\text{H}\alpha = 0.25$) in our spectrum also appear enhanced by about a factor of 2 to 3 compared to the regions in Miller & Hodge. Inspection of four other emission regions intersected by our slit, which was $2'$ long, roughly centered on and oriented along the major axis of the galaxy, reveals that one other location (hereafter called “B”) has a spectrum similar to that of the primary peak (hereafter called “A,” whose spectrum is plotted in Fig. 29 of Ho et al. 1995). B is separated from A by $31''$. The remaining three peaks have spectra similar to those of the H II regions studied by Miller & Hodge, the main difference being that $[\text{S II}]$ is somewhat enhanced in our cases. The simplest explanation for the unusual character of spectra A and B is that the emission sampled by our slit at these locations comes *not* predominantly from photoionized gas, but rather from shocked plasma. The other three H II region-like objects, then, owe their enhanced $[\text{S II}]$ emission to a mixture of photoionized and shocked gas. In regions A and B, the simultaneous presence of weak $[\text{O III}]$ and moderately strong $[\text{N II}]$ and $[\text{S II}]$ conforms with the predicted signature of collisional ionization in a metal-poor medium (e.g., Dopita et al. 1984). $[\text{O I}] \lambda 6300$ should also be strong, but unfortunately this line is corrupted by night-sky emission (the galaxy has a small radial velocity). Spectra A and B in IC 2574, in fact, look remarkably like those of the SNRs in two other metal-poor irregular galaxies, IC 1613 and NGC 6822 (Dopita et al. 1984). Plotting our measurements of $[\text{O III}] \lambda\lambda 4959, 5007/\text{H}\beta$ and $[\text{N II}] \lambda\lambda 6548, 6583/\text{H}\alpha$ on Figure 10 of Dopita et al., we deduce that regions A and B have abundances of $\text{O}/\text{H} \approx 0.7 \times 10^{-4}$ and 1.5×10^{-4} , respectively, and $\text{O}/\text{N} \approx 12$ and 24 , respectively. Using $[\text{N II}] \lambda\lambda 6548, 6583/\text{H}\alpha$ and $[\text{S II}] \lambda 6731/\text{H}\alpha$ and Figure 8 of Dopita et al. gives somewhat different values of $\text{O}/\text{H} \approx 0.2 \times 10^{-4}$ and $\text{O}/\text{N} \approx 5$ for both regions. However, if the abundance ratio of sulfur to oxygen were to be increased by a factor of 2, which is within the range of variation observed in SNRs (Dopita et al. 1984), O/H and O/N would be higher, and the abundances deduced from the two diagnostic diagrams would be in agreement with each other. The oxygen and nitrogen abundances derived from the shocked regions in IC 2574 agree very well with Miller & Hodge’s determination based on the analysis of its H II regions ($\text{O}/\text{H} \approx 1.4 \times 10^{-4}$ and $\text{O}/\text{N} \approx 30$), and are consistent with abundances established in late-type galaxies (e.g., Garnett 1990).

5. Summary

H II regions are frequently found in the central few hundred parsecs of disk galaxies. A substantial fraction (42%) of all spirals in a magnitude-limited survey of nearby galaxies contain “H II nuclei,” with the detection rate of these objects rising steeply toward galaxies with late Hubble types.

The physical properties of H II nuclei in some respects resemble those of giant H II regions in spiral disk, but differ in several others. The two classes of H II regions generally have similar $H\alpha$ luminosities, electron densities, and ionized hydrogen masses, but H II nuclei are characterized by higher oxygen abundances, somewhat higher internal extinctions, and much smaller volume filling factors. The emission-line equivalent widths of typical H II nuclei are also very small because of the strong dilution from the composite, and generally much older, stellar population of the nuclei.

As first recognized by Kennicutt et al. (1989), H II nuclei distinguish themselves spectroscopically from disk H II regions by their stronger low-ionization forbidden emission. We verified this trend for the [N II] $\lambda\lambda 6548, 6583$ and [S II] $\lambda\lambda 6716, 6731$ lines, and, for the first time, also for the weak [O I] $\lambda\lambda 6300, 6364$ transitions. There are several possible explanations for the enhancement of the low-ionization lines in nuclear H II regions. These include: (1) a secondary ionization source from a weak AGN, (2) exceptionally hot stars coupled with nebular conditions in the H II regions that are unique to the nuclear environment, (3) shocks, and (4) the modification of the thermal properties of metal-enriched gas by dust grains. A dominant contribution to the excess low-ionization emission from the diffuse ionized medium seems implausible given the relatively large strength of [O I].

A number of properties of H II nuclei systematically depend on the morphological type of the host galaxy, with the dividing line between “early” and “late” types occurring near Sbc. The most obvious difference between the two groups is their oxygen abundance, the primary parameter controlling the excitation of the line-emitting gas: early-type nuclei on average have low excitation, whereas late-type nuclei have excitations spanning the full observed range. The oxygen abundance inferred from the [O III]/ $H\beta$ ratios indicate $[O/H] \approx (1.1\text{--}3.3) [O/H]_{\odot}$ for early-type systems and $[O/H]$ ranging from $\lesssim 0.25$ to $3.5 [O/H]_{\odot}$ for late-type systems. It is interesting to note that Markarian starburst nuclei generally have rather high excitation, perhaps an indication that these nuclei are experiencing one of their earliest generations of vigorous star formation. A small number of H II nuclei, all in early-type hosts, emit exceptionally strong [N II] lines; nitrogen may be selectively enhanced in these objects. Early-type nuclei have much higher $H\alpha$ luminosities, and hence formation rates of massive stars, than do late-type nuclei. The underlying physical basis for this difference may be linked to the increased effectiveness of bars in driving gaseous inflow in systems with large bulge-to-disk ratios. The early-type systems are additionally more highly reddened, and they possess higher electron densities. Finally, a minority of the late-type spirals contain H II nuclei with exceptionally strong [S II] and [O I] emission. We suggest that shock-wave heating contributes to the excitation in these regions.

The research of L. C. H. is currently funded by a postdoctoral fellowship from the Harvard-Smithsonian Center for Astrophysics. Financial support for this work was provided by NSF grants AST-8957063 and AST-9221365, as well as by NASA grants AR-5291-93A and AR-5792-94A from the Space Telescope Science Institute (operated by AURA, Inc., under NASA contract NAS5-26555). L. C. H. is grateful to Joe Shields and Ian Evans for informative correspondence on H II region models and for providing electronic tabulations of their photoionization calculations. We thank Chris McKee and Hy Spinrad for their critical reading of an earlier draft of the manuscript, and an anonymous referee for several insightful recommendations.

References

- Baldwin, J. A., Phillips, M. M., & Terlevich, R. 1981, *PASP*, 93, 5
- Balzano, V. A. 1983, *ApJ*, 268, 602
- Campbell, A. 1988, *ApJ*, 335, 644
- Coziol, R., Demers, S., Barnéoud, R., & Peña, M. 1997, *AJ*, in press
- Dinerstein, H. L. 1990, in *The Interstellar Medium in Galaxies*, ed. H. A. Thronson, & J. M. Shull (Dordrecht: Kluwer), 257
- Dinerstein, H. L., & Shields, G. A. 1986, *ApJ*, 311, 45
- Domgörgen, H., & Mathis, J. S. 1994, *ApJ*, 428, 647
- Dopita, M. A., Binette, L., D’Odorico, S., & Benvenuti, P. 1984, *ApJ*, 276, 653
- Edmunds, M. G., & Pagel, B. E. J. 1984, *MNRAS*, 211, 507
- Evans, I. N., & Dopita, M. A. 1985, *ApJS*, 58, 125
- Filippenko, A. V., & Sargent, W. L. W. 1985, *ApJS*, 57, 503
- Filippenko, A. V., & Terlevich, R. 1992, *ApJ*, 397, L79
- French, H. B. 1980, *ApJ*, 240, 41
- Garnett, D. R. 1990, *ApJ*, 363, 142
- Greenawalt, B., Walterbos, R. A. M., & Braun, R. 1997, *ApJ*, in press
- Heckman, T. M. 1980a, *A&A*, 87, 142
- Heckman, T. M. 1980b, *A&A*, 87, 152
- Heckman, T. M., Balick, B., & Crane, P. C. 1980, *A&AS*, 40, 295
- Heckman, T. M., van Breugel, W. J. M., Miley, G. K., & Butcher, H. R. 1983, *AJ*, 88, 1077
- Helfer, T. T., & Blitz, L. 1993, *ApJ*, 419, 86
- Ho, L. C. 1996, in *The Physics of LINERs in View of Recent Observations*, ed. M. Eracleous, et al. (San Francisco: ASP), 103
- Ho, L. C., Filippenko, A. V., & Sargent, W. L. W. 1993, *ApJ*, 417, 63
- Ho, L. C., Filippenko, A. V., & Sargent, W. L. W. 1995, *ApJS*, 98, 477
- Ho, L. C., Filippenko, A. V., & Sargent, W. L. W. 1996, in *The Interplay Between Massive Star Formation, the ISM and Galaxy Evolution*, ed. D. Kunth, et al. (Gif-sur-Yvette: Editions Frontières), 341
- Ho, L. C., Filippenko, A. V., & Sargent, W. L. W. 1997a, *ApJS*, in press
- Ho, L. C., Filippenko, A. V., & Sargent, W. L. W. 1997b, *ApJ*, in press
- Ho, L. C., Filippenko, A. V., & Sargent, W. L. W. 1997c, *ApJ*, in press
- Israel, F. P., & Kennicutt, R. C. 1980, *Astron. Lett.*, 21, 1
- Kaufman, M., Bash, F. N., Kennicutt, R. C., & Hodge, P. W. 1987, *ApJ*, 319, 61
- Keel, W. C. 1983, *ApJS*, 52, 229
- Keel, W. C. 1984, *ApJ*, 282, 75

- Kenney, J. D. 1996, in IAU Colloq. 157, Barred Galaxies, ed. R. Buta, B. G. Elmegreen, & D. A. Crocker (San Francisco: ASP), 150
- Kennicutt, R. C. 1984, ApJ, 287, 116
- Kennicutt, R. C. 1988, ApJ, 334, 144
- Kennicutt, R. C. 1992, ApJS, 79, 255
- Kennicutt, R. C., Keel, W. C., & Blaha, C. A. 1989, AJ, 97, 1022 (KKB)
- Kunth, D., & Sargent, W. L. W. 1983, ApJ, 273, 81
- Lehnert, M. D., & Heckman, T. M. 1994, ApJ, 426, L27
- Mathis, J. 1986, PASP, 98, 995
- Mathis, J. 1990, ARA&A, 28, 37
- Mazzarella, J. M., & Balzano, V. A. 1986, ApJS, 62, 751
- McCall, M. L., Rybski, P. M., & Shields, G. A. 1985, ApJS, 57, 1
- McGaugh, S. S. 1991, ApJ, 380, 140
- Miller, B. W., & Hodge, P. 1996, ApJ, 458, 467
- Oey, M. S., & Kennicutt, R. C. 1993, ApJ, 411, 137
- Pagel, B. E. J., Edmunds, M. G., Blackwell, D. E., Chun, M. S., & Smith, G. 1979, MNRAS, 189, 95
- Peimbert, M., & Torres-Peimbert, S. 1992, A&A, 253, 349
- Phillips, A. P., Gondhalekar, P. M., & Pettini, M. 1982, MNRAS, 200, 687
- Pogge, R. W. 1989, ApJS, 71, 433
- Press, W. H., Flannery, B. P., Teukolsky, S. A., & Vetterling, W. T. 1986, Numerical Recipes, the Art of Scientific Computing (Cambridge: Cambridge Univ. Press)
- Rand, R. J. 1996, in The Interplay Between Massive Star Formation, the ISM and Galaxy Evolution, ed. D. Kunth, et al. (Gif-sur-Yvette: Editions Frontières), 515
- Reynolds, J. S. 1990, in I.A.U. Symp. 144, The Interstellar Disk/Halo Connection in Galaxies, ed. H. Bloemen (Dordrecht: Kluwer), 67
- Roberts, M. S., & Haynes, M. P. 1994, ARA&A, 32, 115
- Ryder, S. D. 1995, ApJ, 444, 610
- Sandage, A. R., & Tammann, G. A. 1981, A Revised Shapley-Ames Catalog of Bright Galaxies (Washington, DC: Carnegie Institute of Washington)
- Shields, G. A. 1990, ARA&A, 28, 525
- Shields, G. A., & Tinsley, B. M. 1976, ApJ, 203, 66
- Shields, J. C. 1992, ApJ, 399, L27
- Shields, J. C., & Filippenko, A. V. 1990, AJ, 100, 1034
- Shields, J. C., & Kennicutt, R. C., Jr. 1995, ApJ, in 454, 807
- Shull, J. M., & McKee, C. F. 1979, ApJ, 227, 131

- Spergel, D. N., & Blitz, L. 1992, *Nature*, 357, 665
- Stauffer, J. R. 1981, Ph.D. thesis, University of California, Berkeley
- Stauffer, J. R. 1982, *ApJS*, 50, 517
- Terlevich, R., Melnick, J., Masegosa, J., Moles, M., & Copetti, M. V. F. 1991, *A&AS*, 91, 285
- Turnrose, B. E. 1976, *ApJ*, 210, 33
- van der Hulst, J. M., Kennicutt, R. C., Crane, P. C., & Rots, A. H. 1988, *A&A*, 195, 38
- Veilleux, S., & Osterbrock, D. E. 1987, *ApJS*, 63, 295
- Véron, P., & Véron-Cetty, M.-P. 1986, *A&A*, 161, 145
- Véron, P., Véron-Cetty, M.-P., Bergeron, J., & Zuiderwijk, E. J. 1981, *A&A*, 97, 71
- Vílchez, J. M., & Pagel, B. E. J. 1988, *MNRAS*, 231, 257
- Zaritsky, D., Elston, R., & Hill, J. M. 1990, *AJ*, 99, 1108

Figure Captions

Fig. 1. — Integrated absolute blue magnitudes (M_{BT}^0 , corrected for internal extinction; Ho et al. 1997a) of the host galaxies of H II nuclei for (a) all Hubble types (excluding peculiar classifications), (b) types ranging from S0 to Sbc, and (c) types ranging from Sc to I0. The bins are separated by 0.5 mag.

Fig. 2. — H α luminosities [L(H α)] for (a) all H II nuclei in our survey observed under photometric conditions, (b) nuclei with types S0–Sbc, (c) nuclei with types Sc–I0, (d) starburst nuclei from Balzano (1983), and (e) first-ranked disk H II regions from Kennicutt (1988). Each bin corresponds to 0.25 in logarithmic units. Our survey luminosities were corrected for internal and Galactic reddening, estimated from the observed H α /H β ratio, using a Galactic extinction curve (see Ho et al. 1997a). Since Balzano’s individual Balmer decrement values are rather uncertain, her luminosities were dereddened using their median H α /H β ratio, which corresponds to $E(B - V) = 0.62$ mag. The L(H α) values for the disk H II regions represent the average luminosity of the three first-ranked regions as tabulated by Kennicutt, who only corrected for Galactic reddening. We dereddened the luminosities by $E(B - V) = 0.29$ mag, the median internal reddening of our compilation of disk H II regions.

Fig. 3. — H β emission equivalent widths for (a) all H II nuclei in our survey, (b) nuclei with types S0–Sbc, (c) nuclei with types Sc–I0, and (d) the sample of disk H II regions of McCall et al. (1985). The bins are separated by 5 Å, and the last bin contains all objects with $EW(H\beta) > 99$ Å.

Fig. 4. — Distribution of internal reddening [$E(B - V)_{\text{int}}$] for (a) all H II nuclei in our survey, (b) nuclei with types S0–Sbc, (c) nuclei with types Sc–I0, and (d) the sample of disk H II regions of McCall et al. (1985). The bins are separated by 0.1 mag. We estimated the internal reddening in our measurements from the observed H α /H β ratio (see Ho et al. 1997a).

Fig. 5. — Electron densities (n_e) derived from the [S II] $\lambda 6716/\lambda 6731$ ratio for (a) all H II nuclei in our survey, (b) nuclei with types S0–Sbc, (c) nuclei with types Sc–I0, and (d) the sample of disk H II regions of McCall et al. (1985). The bins are separated by 50 cm $^{-3}$.

Fig. 6. — Extinction-corrected [O III] $\lambda 5007/H\beta$ ratios for (a) all H II nuclei in our survey, (b) nuclei with types S0–Sbc, (c) nuclei with types Sc–I0, (d) starburst nuclei from Balzano (1983), and (e) disk H II regions from several sources. The bins are separated by units of 0.2.

Fig. 7. — Diagnostic diagram, adapted from Veilleux & Osterbrock (1987), plotting $\log [O \text{ III}] \lambda 5007/H\beta$ versus $\log [N \text{ II}] \lambda 6583/H\alpha$. The symbols have the following meaning: *solid circles* = disk H II regions, *open circles* = H II nuclei, and *asterisks* = starburst nuclei. The *dashed curve* denotes the theoretical models of disk H II regions by McCall et al. (1985). The calculations assume that the effective temperature of the ionizing stars decreases with increasing oxygen abundance, ranging from $T_{\text{eff}} = 47,000$ to 38,500 K as $(O/H)/(O/H)_{\odot}$ varies from 0.5 to 3.5 (*top to bottom*). Also shown are the photoionization models of Shields & Kennicutt (1995) which incorporate the effects of dust (*dotted curves*); the top curve was calculated for $T_{\text{eff}} = 45,000$ K and the bottom one for $T_{\text{eff}} = 38,000$ K. The models assume a constant density and ionization parameter, with abundances varying between 0.1 and 5 times the solar values from the

upper left to the bottom right of each curve. The unusual object IC 2574 (see § 4.2) is labeled.

Fig. 8. — Extinction-corrected $[\text{N II}] \lambda 6583/\text{H}\alpha$ ratio for (a) all H II nuclei in our survey, (b) nuclei with types S0–Sbc, (c) nuclei with types Sc–I0, (d) starburst nuclei from Balzano (1983), and (e) disk H II regions from several sources. The bins are separated by units of 0.05.

Fig. 9. — Diagnostic diagram plotting $\log [\text{O III}] \lambda 5007/\text{H}\beta$ versus $\log [\text{N II}] \lambda 6583/\text{H}\alpha$ for (*solid circles*) early-type (S0–Sbc) H II nuclei and (*open circles*) late-type (Sc–I0) H II nuclei. The curve denotes the theoretical models of disk H II regions by McCall et al. (1985) described in the caption of Figure 7. The unusual object IC 2574 (see § 4.2) is labeled.

Fig. 10. — Diagnostic diagram plotting $\log [\text{O III}] \lambda 5007/\text{H}\beta$ versus $\log [\text{S II}] \lambda\lambda 6716, 6731/\text{H}\alpha$. The symbols have the same meaning as in Figure 7.

Fig. 11. — Extinction-corrected $[\text{S II}] \lambda\lambda 6716, 6731/\text{H}\alpha$ ratio for (a) all H II nuclei in our survey, (b) nuclei with types S0–Sbc, (c) nuclei with types Sc–I0, (d) starburst nuclei from Balzano (1983), and (e) disk H II regions from several sources. The bins are separated by units of 0.05.

Fig. 12. — Diagnostic diagram plotting $\log [\text{O III}] \lambda 5007/\text{H}\beta$ versus $\log [\text{S II}] \lambda\lambda 6716, 6731/\text{H}\alpha$ for (*solid circles*) early-type (S0–Sbc) H II nuclei and (*open circles*) late-type (Sc–I0) H II nuclei. The curve denotes the theoretical models of disk H II regions by McCall et al. (1985) described in the caption of Figure 7.

Fig. 13. — Diagnostic diagram plotting $\log [\text{O III}] \lambda 5007/\text{H}\beta$ versus $\log [\text{O I}] \lambda 6300/\text{H}\alpha$. The symbols have the following meaning: *open triangles* = disk H II regions, *solid circles* = early-type (S0–Sbc) H II nuclei, *open circles* = late-type (Sc–I0) H II nuclei, and *asterisks* = starburst nuclei. The curves denote the theoretical models of disk H II regions described in the caption of Figure 7.

Fig. 14. — Extinction-corrected $[\text{O I}] \lambda 6300/\text{H}\alpha$ ratio for (a) all H II nuclei in our survey, (b) nuclei with types S0–Sbc, (c) nuclei with types Sc–I0, (d) starburst nuclei from Balzano (1983), and (e) disk H II regions from several sources. The bins are separated by units of 0.01.

Fig. 15. — The line ratios $[\text{S II}] \lambda\lambda 6716, 6731/\text{H}\alpha$ and $[\text{O I}] \lambda 6300/\text{H}\alpha$ correlate well with each other. *Solid circles* denote early-type (S0–Sbc) H II nuclei, and *open circles* denote late-type (Sc–I0) H II nuclei.

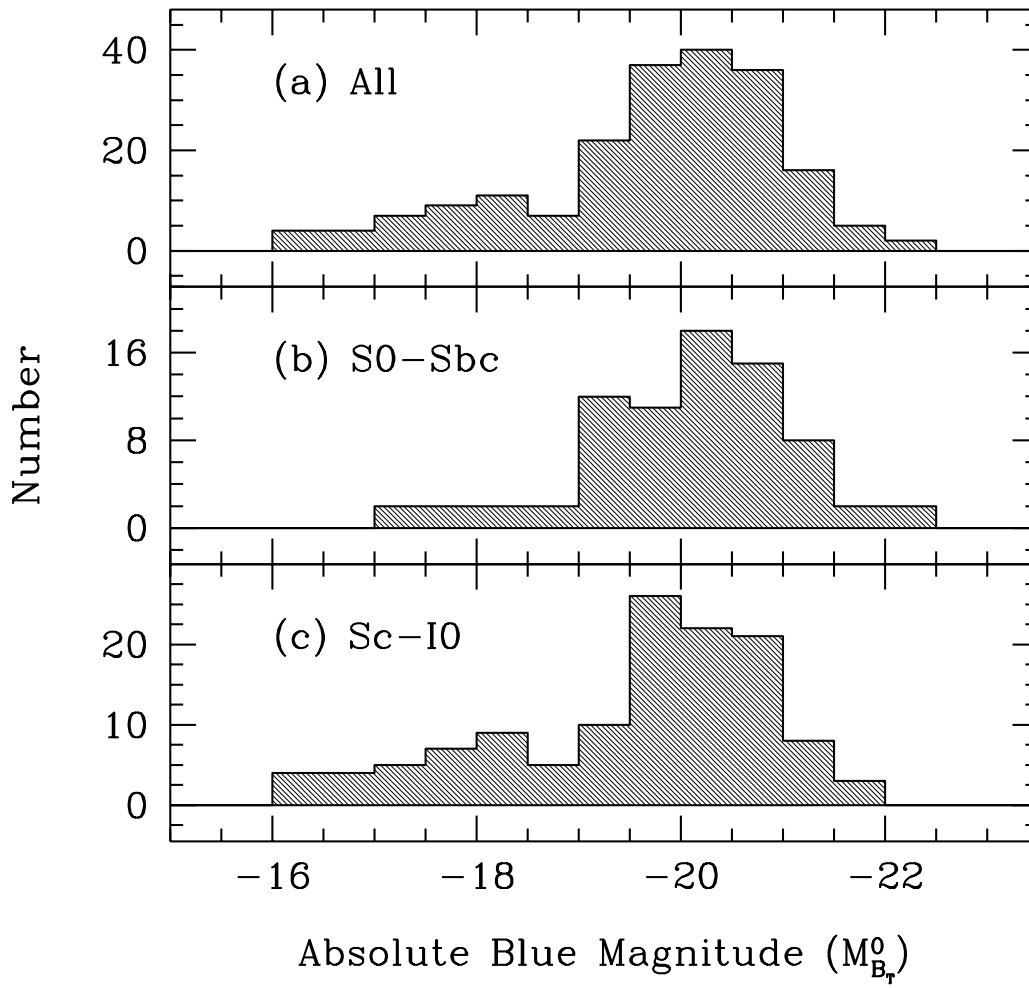


Fig. 1.—

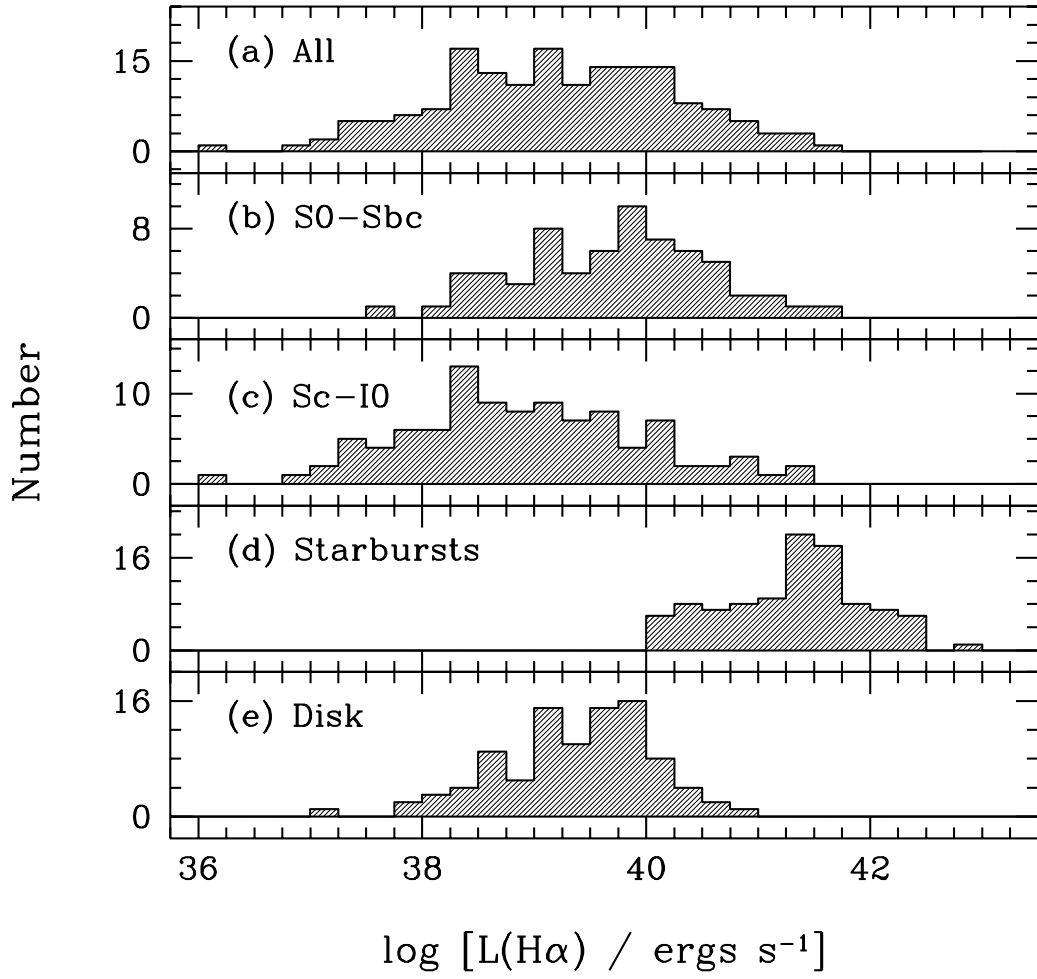


Fig. 2.—

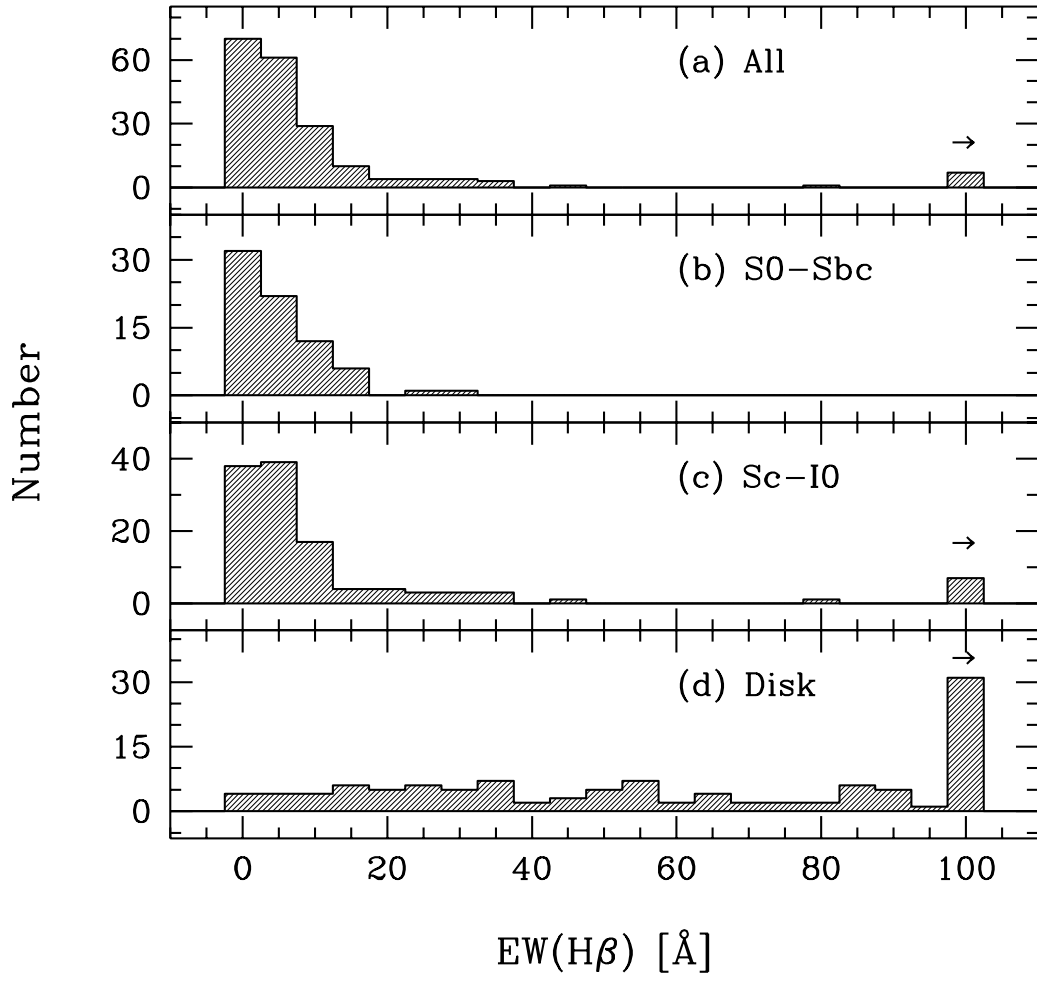


Fig. 3.—

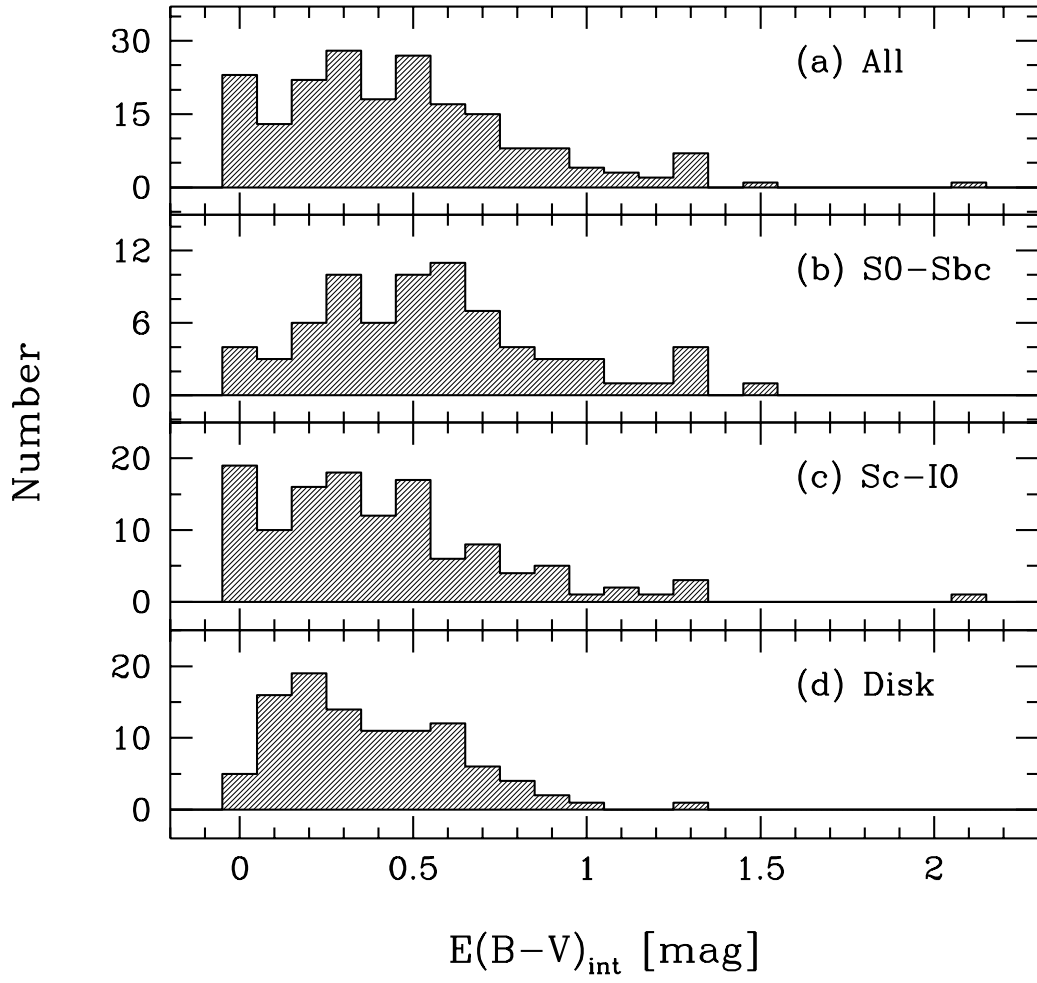


Fig. 4.—

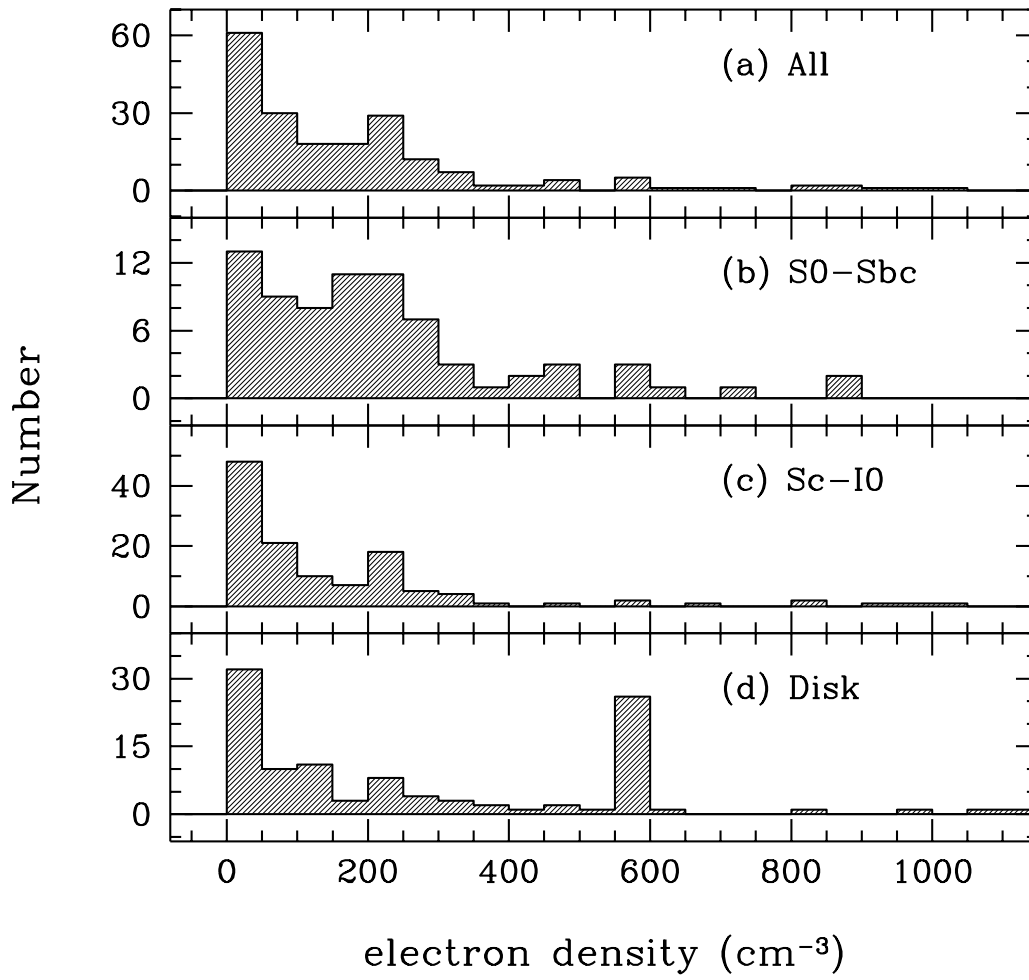


Fig. 5.—

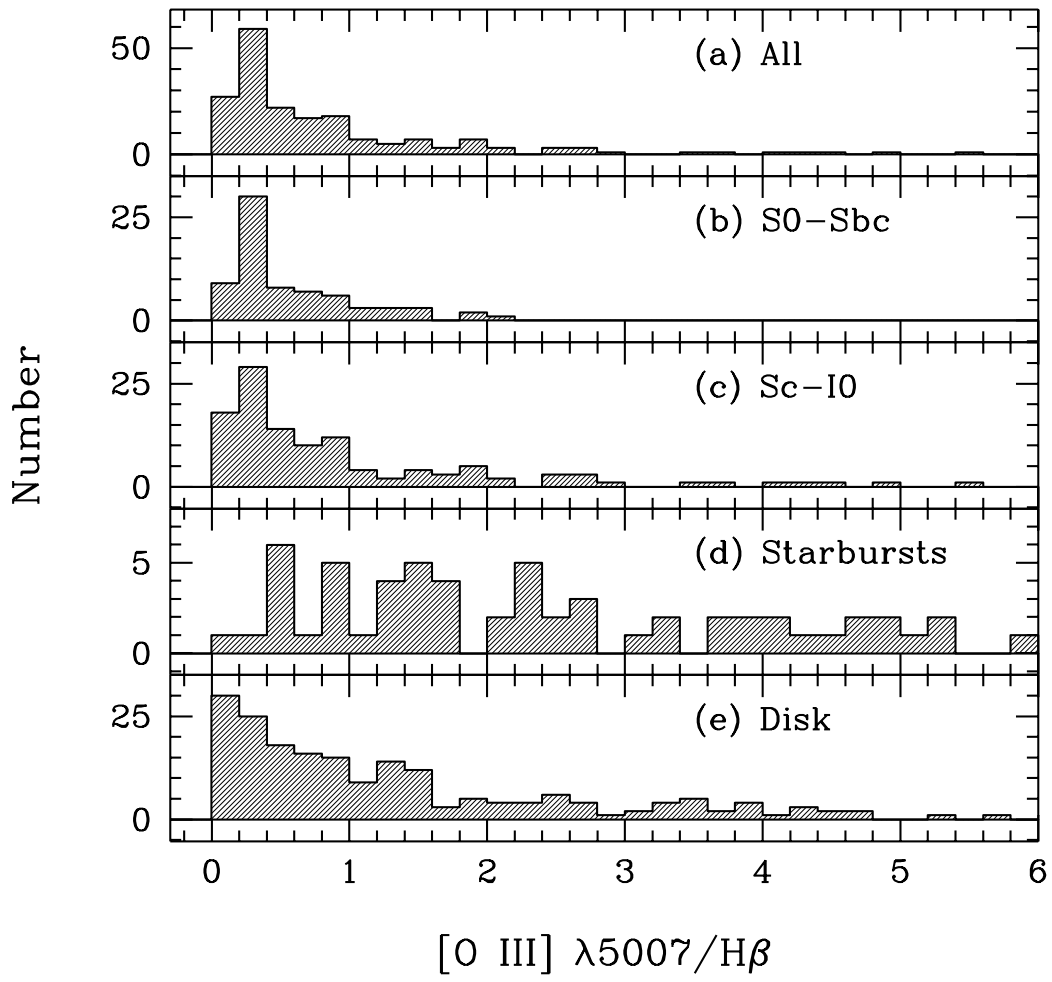


Fig. 6.—

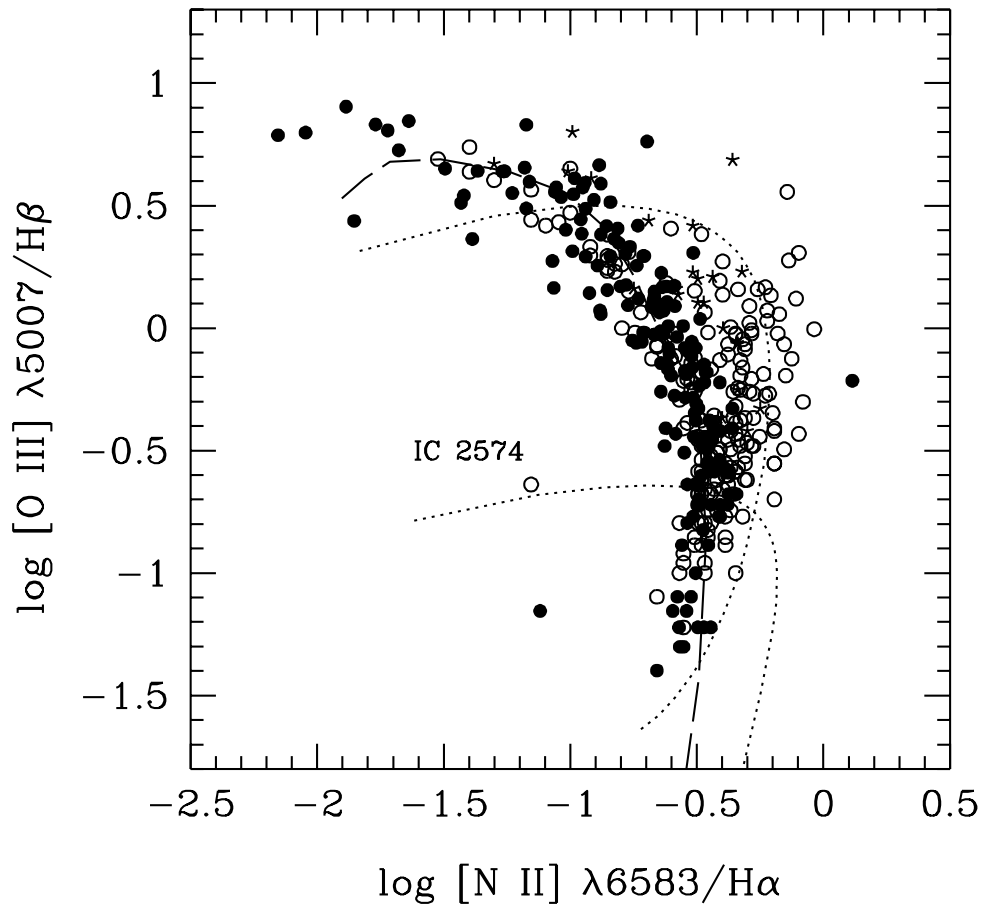


Fig. 7.—

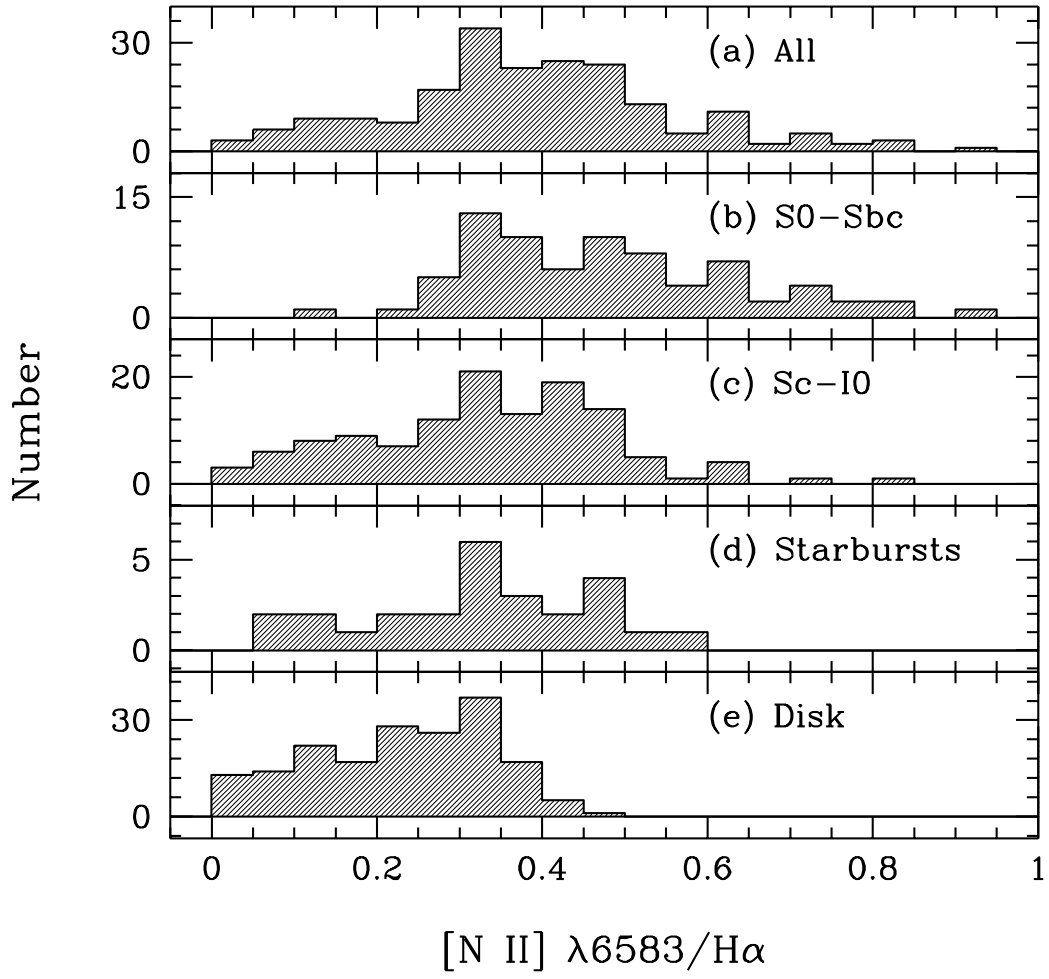


Fig. 8.—

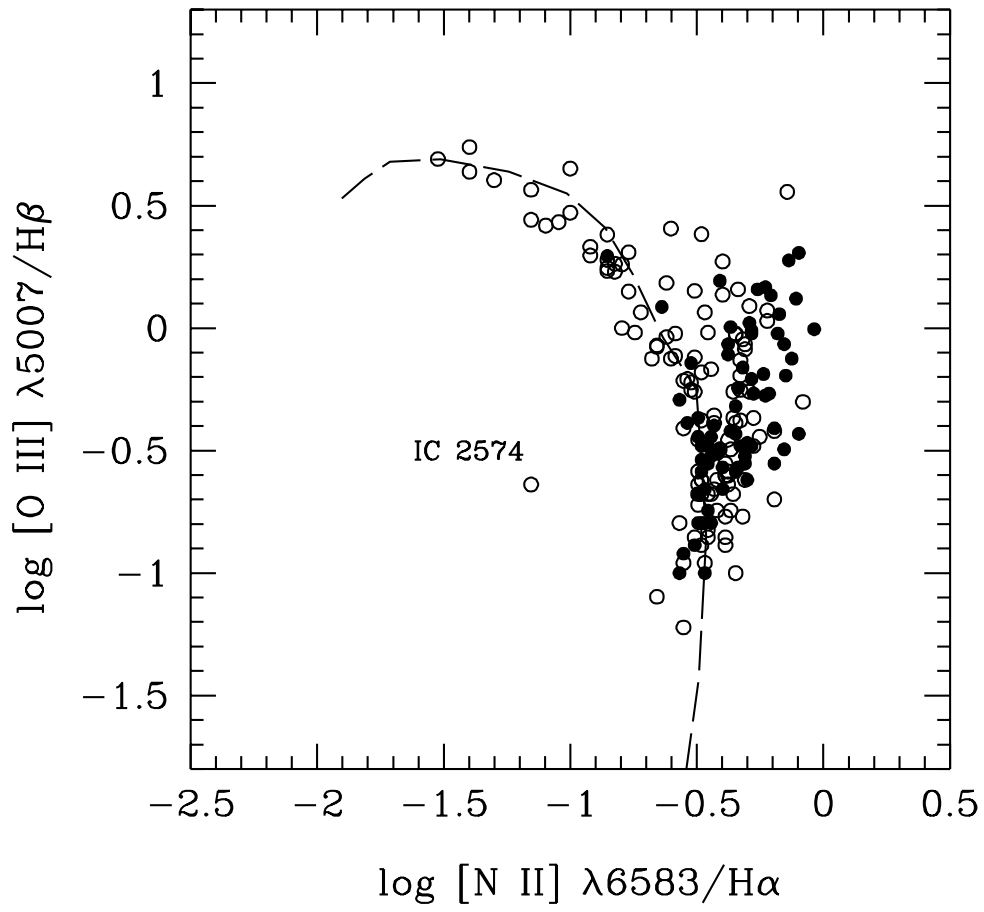


Fig. 9.—

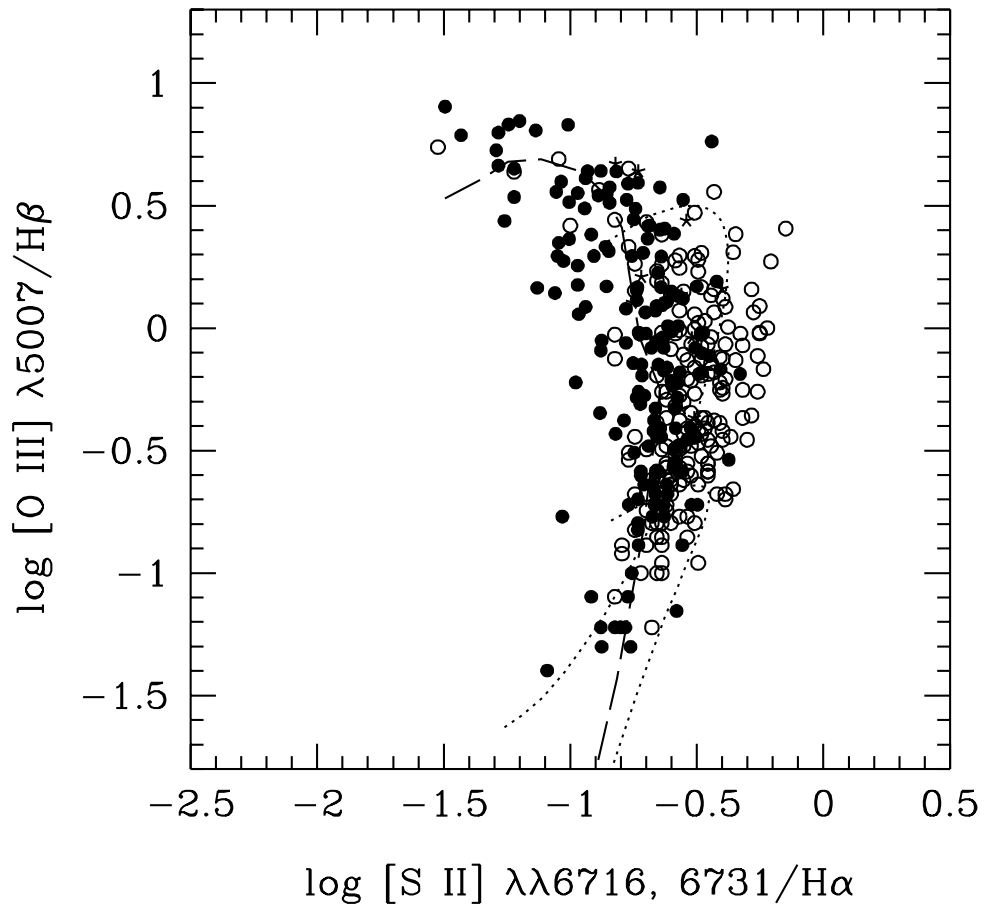


Fig. 10.—

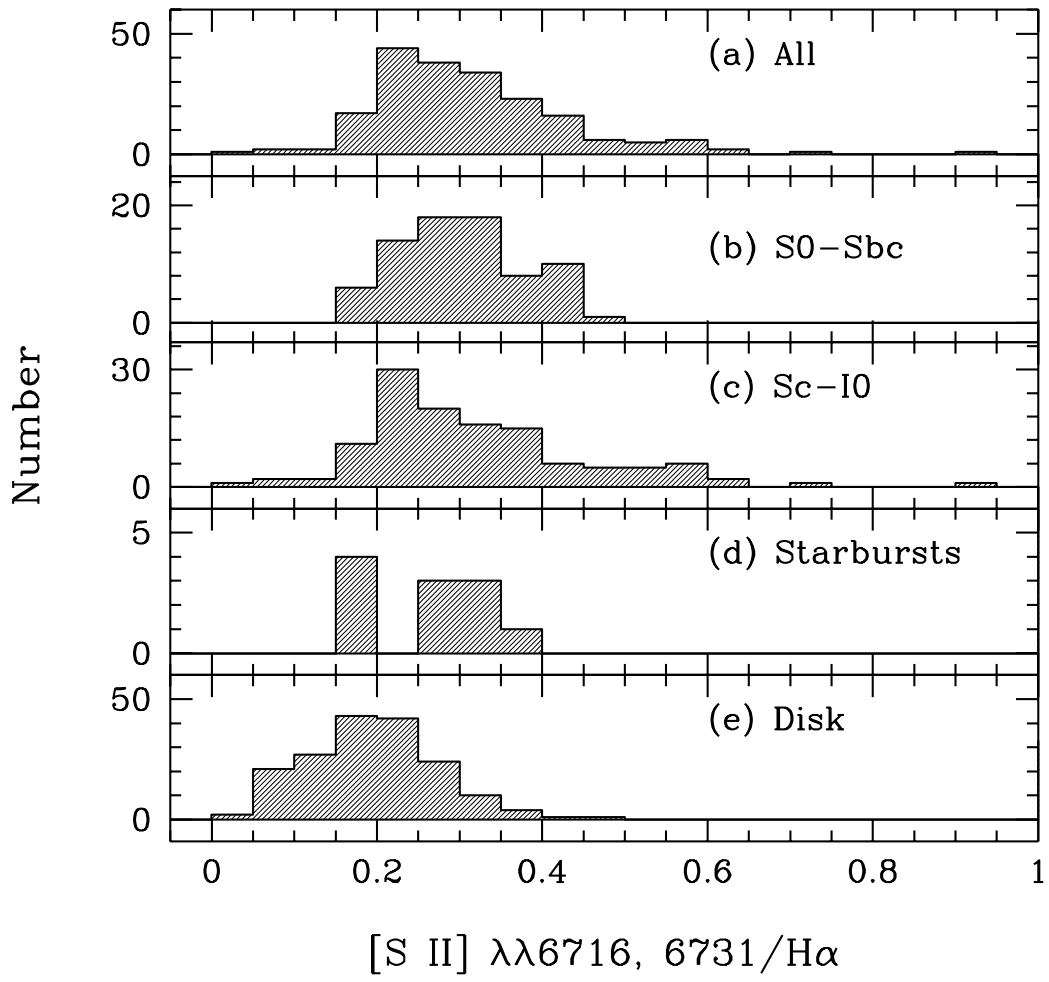


Fig. 11.—

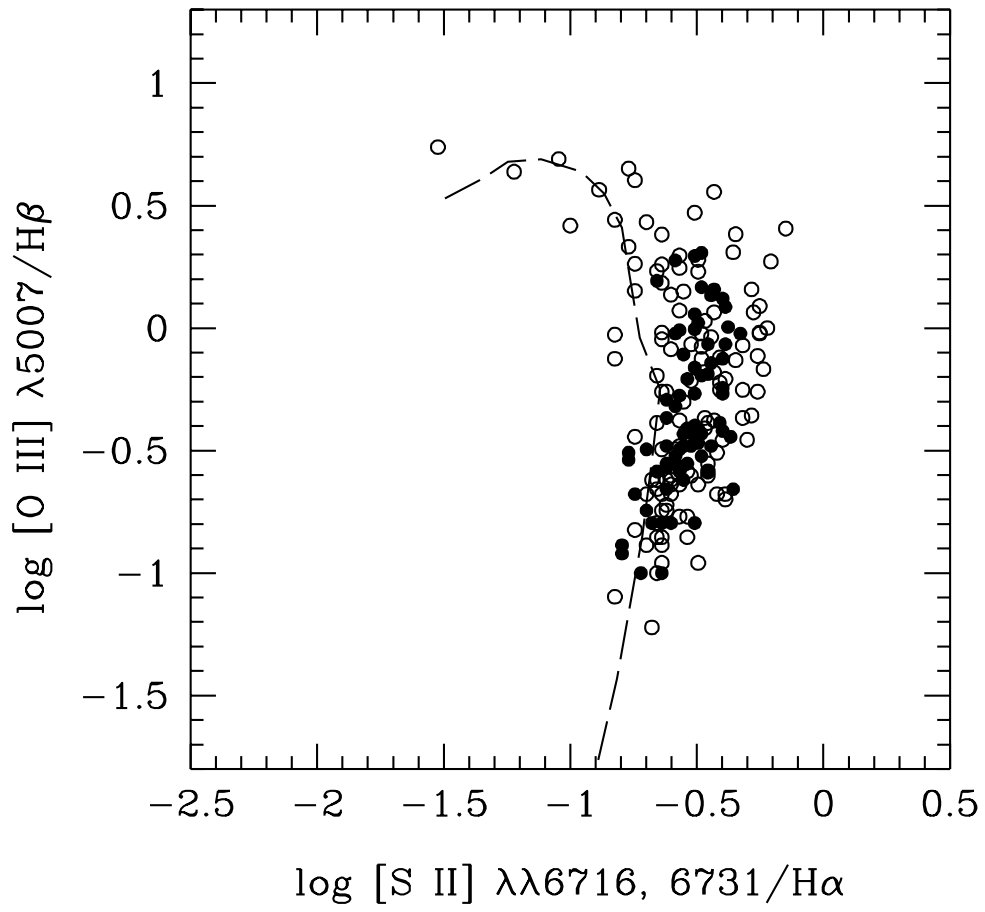


Fig. 12.—

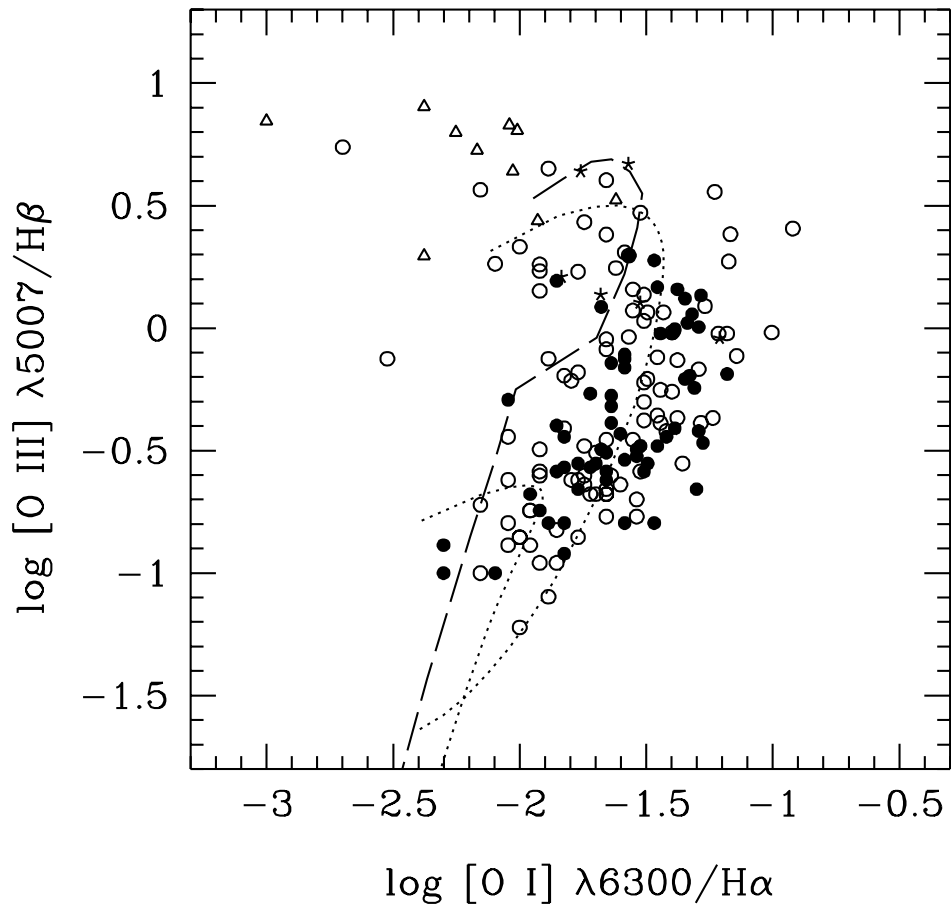


Fig. 13.—

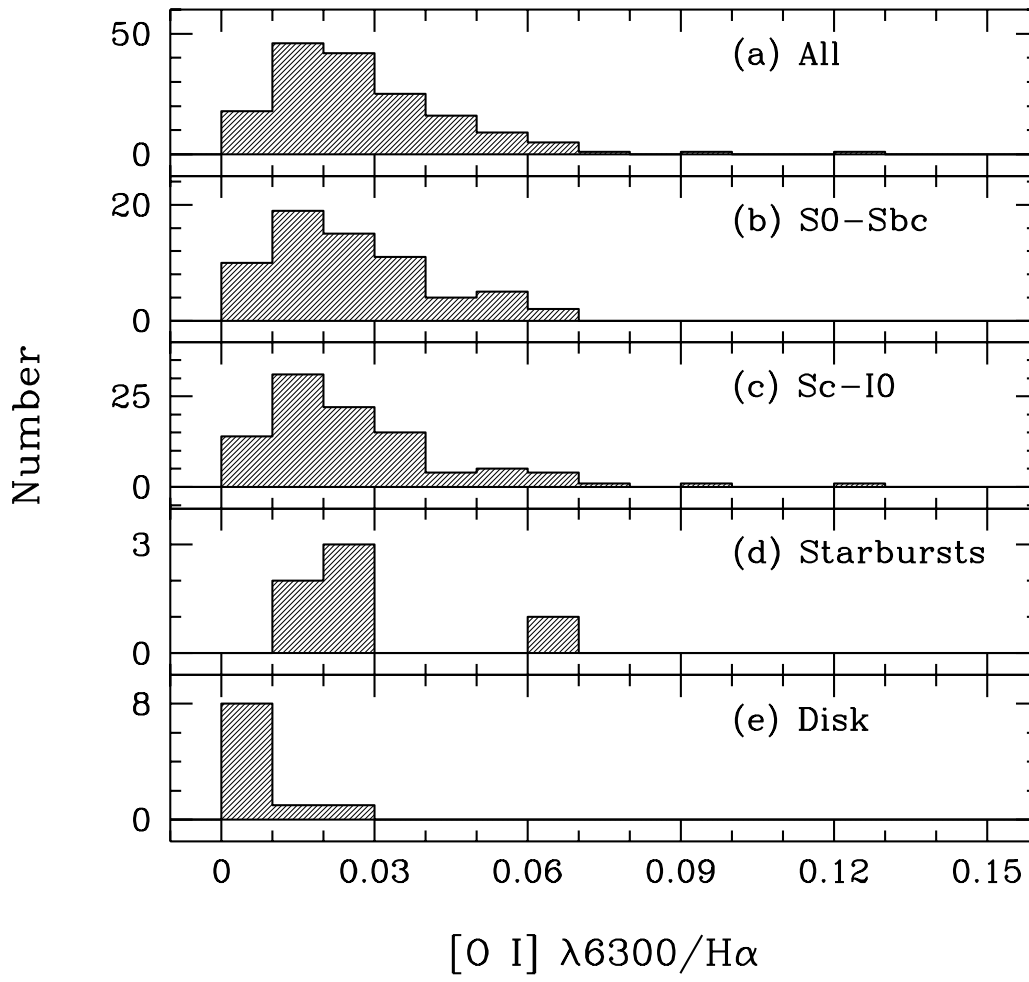


Fig. 14.—

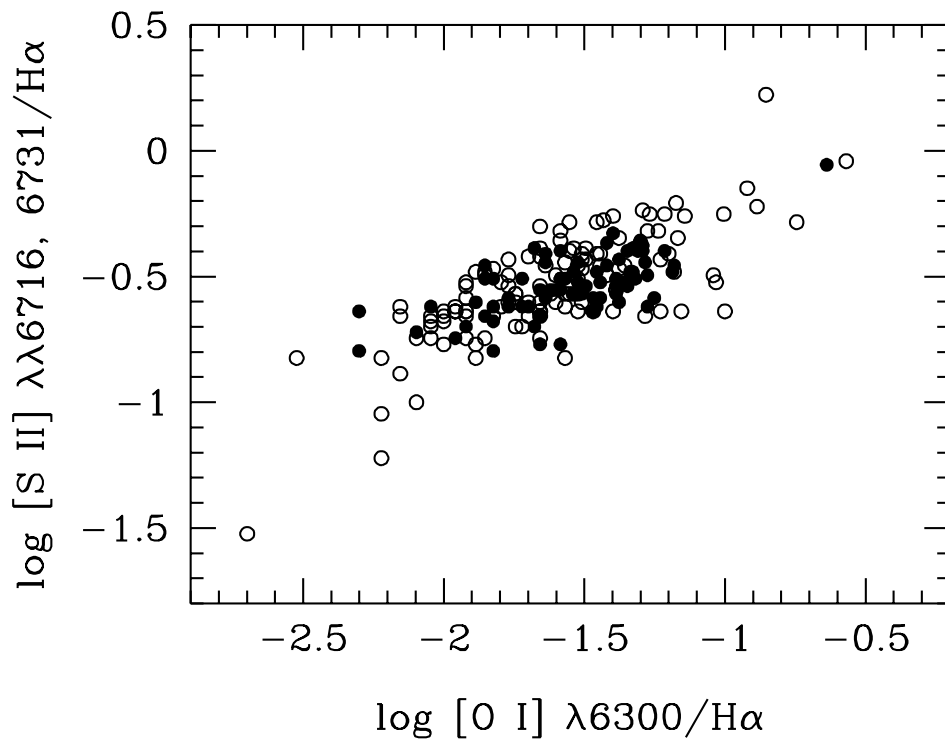


Fig. 15.—